



University Politehnica of Bucharest  
Doctoral School of Materials Science and Engineering



## **PhD THESIS SUMMARY**

# **FUNCTIONALIZED MAGNETIC NANOPARTICLES USED IN THE TREATMENT OF OSTEOARTICULAR DISEASES**

**PhD Student: Alexandru CERNEA**

**Scientific coordinator: Prof. Habil. Dr. Ing. Iulian Vasile ANTONIAC**

**Bucharest, iulie 2020**

## Thanks

At the end of this important stage in my life, I want to address a few words of thanks to those who guided me and gave me support during my doctoral thesis.

Cordial thanks and special gratitude to my doctoral supervisor, Mr. prof.univ.habil.dr.ing. Vasile Iulian Antoniac, from Polytechnic University of Bucharest, for the competent and permanent guidance during the elaboration and realization of this doctoral thesis. I also thank him for his support in writing scientific articles published in specialty magazines.

Thanks to the chairman of the doctoral committee, Mr. prof.univ.habil.dr.ing. Florin Miculescu and the distinguished official referrers: Mr. prof.univ.dr.ing. Corneliu Munteanu, Technical University of Iași, Mr. prof.univ.dr.ing. Cătălin Popa, Technical University of Cluj-Napoca and Mrs. prof.univ.habil.dr.ing. Brândușa Ghiban, from the Polytechnic University of Bucharest, for the honor given to review this paper.

This doctoral thesis would not have been complete without the essential help of the following collaborators: C.S.II.dr.ing. Cristian Petcu from INCDCP ICECHIM Bucharest; prof.univ.dr.ing. Diana Popescu from the Faculty of Industrial Engineering and Robotics, Polytechnic University of Bucharest and prof.univ.dr.ing. Alexandru Morega from the Faculty of Electrical Engineering, Polytechnic University of Bucharest. Thank you for your time, help, and valuable scientific advice.

Cordial thanks to Mrs. conf.dr.med. Rodica Marinescu and Dr. med. Dan Laptoiu from the Colentina Clinical Hospital, Bucharest for the support provided in the realization of this thesis and the identification of the aspects regarding the functionality and clinical applicability of the research carried out within the present paper.

All my love, respect and gratitude, to all my professors during my faculty and master's courses, those who gave me their knowledge and directed me to the field of scientific research.

With special gratitude and love, I dedicate this thesis to my family, who was with me and supported me in all respects during this period.

## **CONTENTS**

Introduction .....	1
<b>CHAPTER 4: MATERIALS, ANALYSIS TECHNIQUES, TEST METHODS AND EXPERIMENTAL EQUIPMENT USED.....</b>	<b>2</b>
4.1. PhD thesis purpose .....	2
4.2. Experimental materials used and work plan .....	3
4.3. Analysis techniques, test methods and equipment used .....	4
<b>CHAPTER 5: SYNTHESIS, FUNCTIONALIZATION AND CHARACTERIZATION OF DRUG-CARRYING MAGNETIC NANOPARTICLES .....</b>	<b>4</b>
5.1. Synthesis and functionalization of drug-carrying magnetic nanoparticles.....	4
5.2. Characterization of drug-carrying magnetic nanoparticles.....	7
5.2.1. Morphological and structural characterization by scanning electron microscopy - SEM and transmission electron microscopy - TEM .....	7
5.2.2. Fourier Transform Infrared Spectroscopy (FT-IR) determinations.....	8
5.2.3. Determination of nanoparticle sizes and zeta potential of experimental samples by DLS methods.....	10
<b>CHAPTER 6: TESTING OF VISCOELASTIC SOLUTIONS .....</b>	<b>12</b>
6.1. Rheological testing of improved viscoelastic solutions with drug-carrying magnetic nanoparticles .....	12
6.2. Testing the magnetic properties of improved viscoelastic solutions with drug-carrying magnetic nanoparticles .....	15
6.2.1. Using the COMSOL modeling program.....	15
6.2.2. Testing the effect of permanent magnets on fluid with magnetic nanoparticles....	26
6.3. Testing the biocompatibility of enhanced viscoelastic solutions with drug-carrying magnetic nanoparticles .....	29
<b>CHAPTER 7: DESIGN, EXECUTION AND PRACTICAL USE OF THE COMPLEX SYSTEM OF ORTHOSIS WITH PERMANENT MAGNETS ASSOCIATED WITH A VISCOELASTIC SOLUTION ENHANCED WITH FUNCTIONALIZED MAGNETIC NANOPARTICLES.....</b>	<b>31</b>
7.1. Desing of orthosis with permanent magnets .....	31
7.2. How to clinically use the complex system.....	35
<b>C1. GENERAL CONCLUSIONS .....</b>	<b>40</b>
<b>C2. ORIGINAL CONTRIBUTIONS .....</b>	<b>41</b>
<b>C3. PERSPECTIVES FOR FURTHER DEVELOPMENT .....</b>	<b>42</b>
<b>SELECTIVE BIBLIOGRAPHY .....</b>	<b>43</b>

## INTRODUCTION

---

This doctoral thesis is based on the accumulation of the necessary information on the supporting role of various types of orthoses used in case of traumatic or degenerative injuries. In order to treat this subject, elements of applied biomechanics and magnetic field are analyzed to optimize the functional and economic parameters that characterize these devices.

Degenerative diseases of the knee are the main cause of severe pain in the knee joints. Usual treatments such as physical therapy, patient weight loss and drug treatments with simple intra-articular injections or steroids are not enough to treat these diseases, in the sense that in most cases the best result is to attenuate the severe pain.

Knee orthoses are orthopedic devices that have a protective or corrective role on the knee joint. In the case of traumatic or degenerative injuries of the knee joint, orthoses help a faster healing by supporting in a fixed and correct position of the joint, thus having the role of correcting certain bone defects.

Taking into account all these aspects, controlled drug delivery treatments applied together with orthoses are considered to be beneficial for the treatment of knee diseases, having the advantage of long-term therapeutic effects.

The main objective of this paper is to develop a model of orthosis with a modified design that allows the insertion of groups of permanent magnets for therapeutic use, which controls a sterile viscoelastic solution consisting of polymeric compounds deposited in the matrix of functionalized magnetic nanoparticles. This complex system is a relatively new concept in bioactive treatment known as magnetically controlled viscosupplementation.

In order to obtain this device, the present paper must achieve several objectives, namely: the synthesis and functionalization of magnetic iron oxide nanoparticles ( $\text{Fe}_3\text{O}_4$ ) with magnetic properties, biocompatibility and proper functioning; choosing an optimal position of the permanent magnets, so that the magnetic field generated by them directs the magnetic nanoparticles carrying the drug in the desired area; choosing a suitable design of the orthosis that allows the insertion of the magnets in the desired position.

Thus, this doctoral thesis is structured in two main parts that comprise a total of 7 chapters. The first part is a study of literature that includes the first 3 chapters of the paper.

**Chapter 1**, entitled 'Current state of use of biomaterials in the treatment of knee disorders', refers to the functioning of the knee joint, the diseases that can attack this joint and how to treat them. At the same time, this chapter presents a study of the literature on the current state of the models of knee orthoses used in orthopedics, but also useful information about the viscoelastic solutions on the market used for viscous supplements.

**Chapter 2**, "Magnetic materials with potential applications in medicine", presents the particularities of interest of the magnetic field, magnetic materials that have these properties and types of permanent magnets with applicability in the biomedical field. Because these materials are intended to interact with the human body, the effects generated by the magnetic field on the body are presented.

**Chapter 3** entitled "Magnetic nanoparticles used in the drugs controlled delivery" contains general information about magnetic nanoparticles on their synthesis, methods of production, various ways of functionalization and their applicability in the biomedical field for the controlled delivery of drugs.

After addressing these main themes that underlie the scientific research that characterizes this thesis, we present the experimental research that is divided into the following four main chapters.

**Chapter 4**, entitled “Materials, analysis techniques, test methods and experimental equipment used” refers to the main purpose of the paper and to the detailed presentation of the materials used to obtain the complex device consisting of an orthosis with permanent magnets associated with a viscoelastic solution enhanced with functionalized magnetic nanoparticles. It also presents in detail the analysis techniques of magnet nanoparticles, testing methods of viscoelastic solutions, programs used to simulate magnetic properties to determine the optimal position of magnets and last but not least biocompatibility testing by cytotoxicity tests of these materials.

**Chapter 5** entitled "Synthesis, functionalization and characterization of drug-carrying magnetic nanoparticles" explicitly presents the obtaining method used for the synthesis of nanoparticles, which later, also in these chapters are characterized physically, morphologically and structurally by the techniques presented in the previous chapter.

**Chapter 6** refers to "Testing of viscoelastic solutions" both by rheological methods to highlight the properties of viscoelasticity and by using a mathematical simulation program to determine the optimal position of permanent magnets incorporated in the orthosis, depending on the magnetic field generated by them and the influence on the targeting of nanoparticles in the area of interest.

**Chapter 7** is the final chapter entitled "Design, execution and practical use of the complex system of orthosis with permanent magnets associated with a viscoelastic solution enhanced with functionalized magnetic nanoparticles" and consists in designing the appropriate form of the orthosis taking into account all parameters established until now.

The following are the conclusions reached in this doctoral thesis, as well as personal contributions to it, but also the prospects for further development.

It should be noted that the parameters analyzed in this paper take into account both the characteristics of existing magnets on the market and the properties of properly functionalized magnetic nanoparticle solutions. The study of the behavior of magnetic components aims at concentrating as many magnetic nanoparticles as possible in the antero-patello-femoral area, as well as a greater non-uniformity of the magnetic field generated by the matrix of permanent magnets. In this case, the emphasis is on the origin of magnetism in materials, types of magnetic materials used in contemporary medicine and future applications of magnetic biomaterials.

## **CHAPTER 4: MATERIALS, ANALYSIS TECHNIQUES, TEST METHODS AND EXPERIMENTAL EQUIPMENT USED**

---

### **4.1. PhD thesis purpose**

The study of this paper consists in trying to gather all the information necessary for the correct analysis of the protective, corrective or supportive role of several types of knee orthoses, in order to treat traumatic injuries, but especially degenerative injuries, such as osteoarthritis.

The main objective of this doctoral thesis is to design a complex medical device such as patellofemoral orthoses. The complexity of this orthosis model is represented by the modified design that is intended to be obtained so that it allows the insertion of permanent magnets for therapeutic use in order to control from the outside a sterile viscoelastic solution that is injected into the patient's body. The viscoelastic solution consists of certain functionalized polymeric compounds deposited in the matrix of magnetic nanoparticles (MPN). This technique is a relatively new concept of bioactive treatment, known as bioactive viscous supplementation.

The work is staged in several parts that have individual objectives that must be met in order for the final device to have the optimal functional and mechanical characteristics to be used properly in the treatment of knee diseases.

The first objective is to synthesize, functionalize and then morphologically and structurally characterize the drug-carrying magnetic nanoparticles ideal for their use in combination with a viscoelastic solution. The rheological properties of the improved viscoelastic solution with functionalized magnetic nanoparticles are also tested.

The next goal is to optimally choose the geometric configuration and external positioning of the permanent magnets so that they can interact properly with the viscoelastic solution. The biocompatibility of the drug carrier solution is also monitored.

The last stage consists in designing of orthosis, so that it offers comfort to the patient, but of course, to fulfill its mechanical functions of support, correction or protection of the knee joint. For this, the anatomy of the patient, the dimensions of the device, the chosen position of the permanent magnets, but also the affected area must be taken into account.

The fulfillment of all these objectives during the scientific study leads to satisfactory experimental results, and in this way the design of the complex system consisting of a patello-femoral orthosis associated with permanent magnets that interact with an improved viscoelastic solution with functionalized magnetic nanoparticles is successfully achieved..

## **4.2. Experimental materials used and work plan**

In the present doctoral thesis, different types of experimental materials were used for each component of the complex device of the permanent magnet orthosis type associated with an improved viscoelastic solution with functionalized magnetic nanoparticles.

The first phase of the research focused on the synthesis of magnetic nanoparticles and their functionalization, which was carried out in collaboration with the National Research and Development Institute for Chemistry and Petrochemistry - ICECHIM, Bucharest, by the co-precipitation method.

As raw materials for obtaining magnetic nanoparticles (MNP) were used:

- Hydrated ferrous chloride ( $\text{FeCl}_2 \cdot 4\text{H}_2\text{O}$ );
- Hydrated ferric chloride ( $\text{FeCl}_3 \cdot 6\text{H}_2\text{O}$ );
- Ammonium hydroxide ( $\text{NH}_4\text{OH}$ ) in proportion of 25%;
- Hydrochloric acid of 2M molar concentration.

The following raw materials were used for the functionalization of nanoparticles, which were used without any further purification:

- Tetramethylammonium hydroxide - TMOH (purchased from Fluka); TMOH is used to peptize NMPs, preventing the formation of agglomerations;
- hyaluronic acid - HA (purchased from Sigma Aldrich); HA has the role of functionalizing the MNP solution, to improve the biocompatibility, but also the chemical, biological and therapeutic properties of MPN;
- inulin (purchased from Dahlia tubers, Fluka) - has the role of helping to functionalize MNP by improving functional properties.

Once synthesized and functionalized, the magnetic nanoparticles will be embedded in a viscoelastic solution. Three types of viscoelastic solutions marketed with different sodium hyaluronate concentrations were used in this work, namely:

- Arthrum (A) – 40mg/2ml;
- Jointex Starter (J) – 32mg/2ml;
- NeoVisc (N) – 20mg/2ml.

According to literature data, the concentration of sodium hyaluronate in viscoelastic solutions used in joint therapy is variable, but the concentrations of interest are 40 mg/2ml, 32 mg/2ml and 20 mg/2ml, as well as those used in this paper.

### **4.3. Analysis techniques, test methods and equipment used**

The following techniques were used to characterize and test the synthesized and biofunctionalized magnetic nanoparticles:

*Transmission electron microscopy - TEM* was performed on a TECNAI F30 high-resolution transmission electron microscope to obtain structural and crystallographic information on the surface of magnetic nanoparticles. The main advantage of this method is the possibility to simultaneously obtain the electron diffraction associated with a nanozone and the images of the microstructure in the same sample area.

*Scanning Electron Microscopy – SEM* was used to quantify structural information and to observe and analyze the microstructure (morphology) of magnetic nanoparticles. The analysis was performed on a Quanta 200 scanning electron microscope.

Using *Fourier Transform Infrared Spectroscopy - FT-IR* performed on a JASCO 6200 FT-IR spectrometer, equipped with a attenuated total reflection (ATR) device of the attenuated Golden Gate type, information on the chemical composition of samples was obtained; more precisely, identification of characteristic chemical bonds type and the changes that took place during their operation.

Dynamic Light Scattering - DLS, performed on a Nano Zetasizer device, was used to determine the size and zeta potential (electrokinetic potential in colloidal dispersions) of magnetic nanoparticles dispersed in the viscoelastic solution.

*The rheological tests* were performed with the help of a pair of equipment Rheometer Paar - Physica MC 301 (con-plate configuration, diameter 40 mm), at a temperature of 20°C, in the laboratory REOROM/BIOINGTEH Platform, Polytechnic University of Bucharest (Field Interaction Laboratory - Substance).

*COMSOL software* was used to test the magnetic properties of the permanent magnets used in this application. In this way, the geometric configuration and the optimal positions of the magnets attached to the orthosis are determined and established, which will ensure a proper operation.

The biocompatibility testing of the viscoelastic solution was determined by testing the cytotoxicity of the materials. Cell viability was measured by the MTT assay (3-(4,5-dimethylthiazol-2-yl)-2,5-diphenyltetrazolium bromide) which was purchased from Sigma-Aldrich Corp., St. Louis, MO, USA, America).

## **CHAPTER 5: SYNTHESIS, FUNCTIONALIZATION AND CHARACTERIZATION OF DRUG-CARRYING MAGNETIC NANOPARTICLES**

---

### **5.1. Synthesis and functionalization of drug-carrying magnetic nanoparticles**

Magnetic nanoparticles of iron oxides dispersible in the viscosupplementation solution with a concentration of 32 mg / 2 ml were obtained in accordance with the studies performed, using as raw materials: hydrated ferrous chloride (II) ( $\text{FeCl}_2 \cdot 4\text{H}_2\text{O}$ ), hydrated ferric chloride (III) ( $\text{FeCl}_3 \cdot 6\text{H}_2\text{O}$ ),  $\text{NH}_4\text{OH}$  25% și 2M hydrochloric acid.



*Fig. 5.1: Installation in which the synthesis of magnetic nanoparticles took place: Mechanical stirrer; Thermostat and Nitrogen source under pressure*

The dispersion of iron oxide magnetic nanoparticles was prepared by the classical method of co-precipitation of  $\text{FeCl}_2$  (ferrous chloride) and  $\text{FeCl}_3$  (ferric chloride) to the addition of a concentrated basic solution of ammonium hydroxide (25%  $\text{NH}_4\text{OH}$ ) in a mixture of iron salts in 1:2 molar ratio of  $\text{FeCl}_2:\text{FeCl}_3$ .  $\text{FeCl}_2 \cdot 4\text{H}_2\text{O}$  was dissolved in 2M HCl, and  $\text{FeCl}_3 \cdot 6\text{H}_2\text{O}$  in water. It was mixed in a three-necked flask, stirred mechanically under a nitrogen cushion, and after homogenization the required amount of 25%  $\text{NH}_4\text{OH}$  was added dropwise. The entire mixture was thermostated at  $65^\circ\text{C}$  for one hour and resulted a black precipitate. It was washed 3 times with water, the magnetic particles being attracted to the bottom of the flask with a magnet, and then kept at room temperature for the following uses (peptization and functionalization).

According to previous studies, tetramethylammonium hydroxide - TMOH (Fluka) was used for peptization and hyaluronic acid (Sigma Aldrich), inulin, respectively, (Dahlia tubers, Fluka) + hyaluronic acid (Sigma Aldrich) for functionalization (these raw materials were used without extra purification).

The dispersion of magnetic nanoparticles was used as such or diluted 10, 50 or 100 times for the following steps (which will be found in the coding of the experimental samples).

Next, the magnetic nanoparticles were coated with a layer of TMOH by layer-by-layer technique. After washing the magnetic nanoparticles, a solution of TMOH (1M) was added, which was mixed until homogeneous and then left overnight to allow the peptization phenomenon to take place. The solution thus obtained was stored at room temperature for the following uses.

The next experimental phase consisted of inulin coating, which was used in the formation of the second coating layer of the magnetic nanoparticles. Inulin is a commercial inert polysaccharide that remains neutral to cellular activity. The coating was made simply, also by layer-by-layer method, by mechanical mixing and by ultrasound, respectively. In this case, it was desired that the inulin layer make the transition between magnetic particles, which can have toxic effects on the human body and the final layer of hyaluronic acid. The deposition of hyaluronic acid on nanoparticles was performed by layer-by-layer technique (ultrasound) using two solutions with different concentrations of hyaluronic acid, in order to study the effect of hyaluronic acid concentration on the final properties of biopolymer-magnetic nanoparticles composites.



Fig. 5.2: Ultrasonic device

The purpose of this research was to synthesize a compound that once introduced to the joints of the human body, under the action of an external magnetic field, to give elasticity and suppleness to the cartilage in the desired areas, acting as a "lubricant". For this reason, it was desired to incorporate the synthesized nanoparticles into a final (third) layer of hyaluronic acid. Next were defined the final experimental samples of nanoparticles (table 5.1) that will be introduced into the viscoelastic solution with a concentration of 32mg / 2ml and characterized experimentally.

Table 5.1: Composition of prepared viscoelastic solutions

Samples	Composition
Sample 1	MPN+HA
Sample 2	(MPN+TMOH)
Sample 3	(MPN+TMOH)+HA
Sample 4	(MPN + TMOH) + inulin
Sample 5	((MPN+TMOH)+inulin)+HA
Sample 6	Viscoelastic solution HA concentration 32mg/2ml

MPN – magnetic nanoparticles

TMOH – dispersing agent (tetramethylammonium hydroxide)

INULIN – coating agent

HA – hyaluronic acid

Synthetically, the structure of the experimental magnetic nanoparticles obtained and introduced in the viscoelastic solution with the concentration of 32mg / 2ml is presented in the following figures.

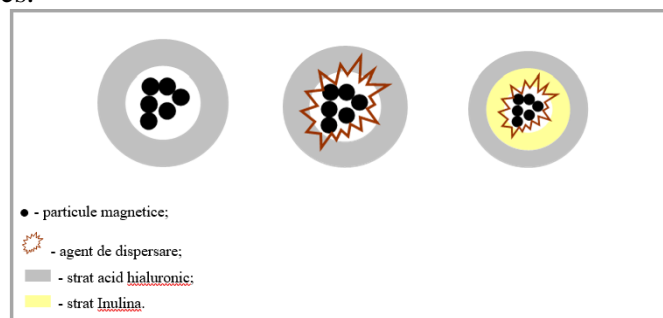


Fig. 5.3: Schematic representation of the obtained functionalized magnetic nanoparticles

The aim was to define two important aspects::

- Optimal variant of functionalization of magnetic nanoparticles (MNP + HA, MNP + TMOH + HA, MNP + TMOH + Inulin + HA);
- Optimal concentration of magnetic nanoparticles.

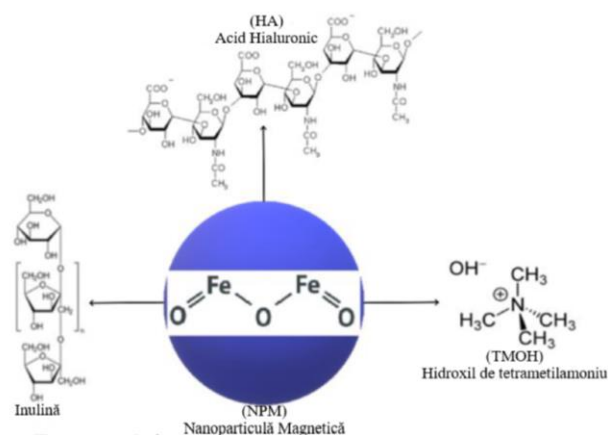


Fig. 5.4: Schematic structure of a functionalized magnetic nanoparticle showing the chemical structure of both magnetic nanoparticles and functionalizing agents [142]

## 5.2. Characterization of drug-carrying magnetic nanoparticles

### 5.2.1. Morphological and structural characterization by scanning electron microscopy - SEM and transmission electron microscopy - TEM

The following figures show the results of SEM - scanning electron microscopy and TEM - transmission electron microscopy investigations.

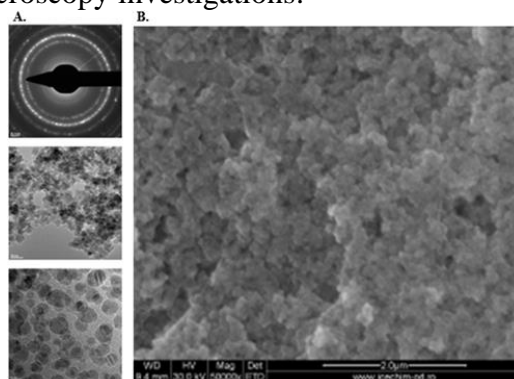


Fig. 5.5: TEM (A) and SEM (B) results for sample 1: MNP + HA

The results of the TEM and SEM analyzes show that in the matrix of the viscoelastic solution, in the initial stage, there are associations of magnetic nanoparticles with asymmetric contour and variable dimensions (figure 5.5.)

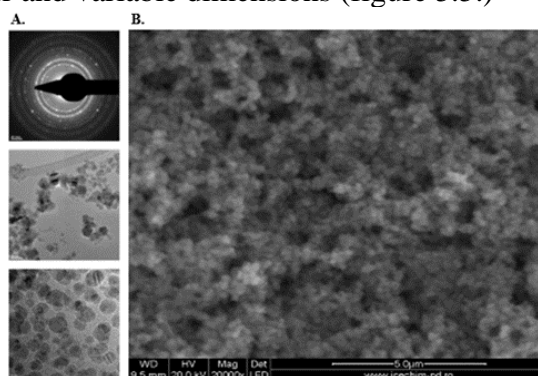


Fig. 5.6: TEM (A) and SEM (B) results for sample 2: (MNP + TMOH)

As a result of the coatings, the shape of the nanoparticles acquires a more uniform distribution. Figure 5.6. shows the magnetic nanoparticles coated with a layer of ammonium

hydroxide (TMOH) and it is shown that the TMOH layer has a beneficial influence as the magnetic nanoparticles become more stable..

The coating with hyaluronic acid (HA) has the same influence on the nanoparticles, which can be seen in figure 5.7. The difference between these two coatings is that after the addition of HA, the contour of the nanoparticles is much better defined.

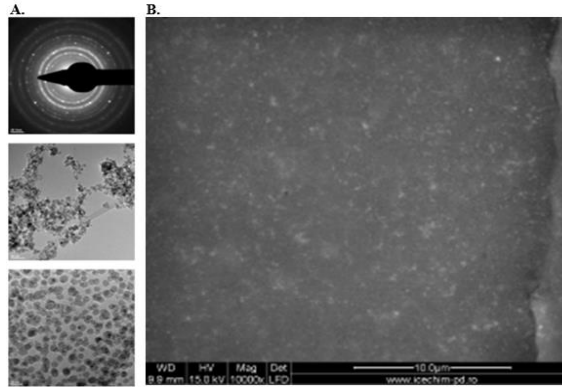


Fig. 5.7: TEM (A) and SEM (B) results for sample 3: (MNP + TMOH) + HA

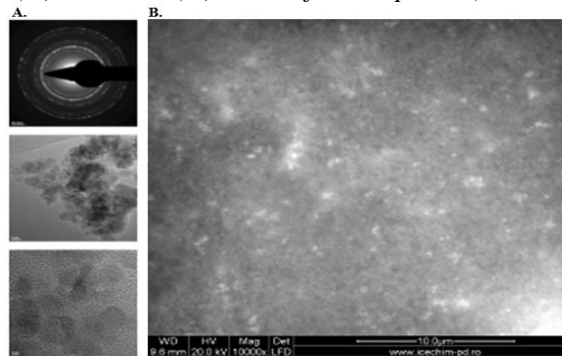


Fig. 5.8: TEM (A) and SEM (B) results for sample 4: (MNP + TMOH) + inulină

The inulin layer is used as a dispersing agent and has the role of preventing the formation of agglomerations of nanoparticles (Figure 5.8.). The final magnetic nanoparticles were successfully incorporated in three layers (TMOH + Inulin + HA) (Figure 5.9.) and led to a uniform distribution of nanoparticles in the viscoelastic solution..

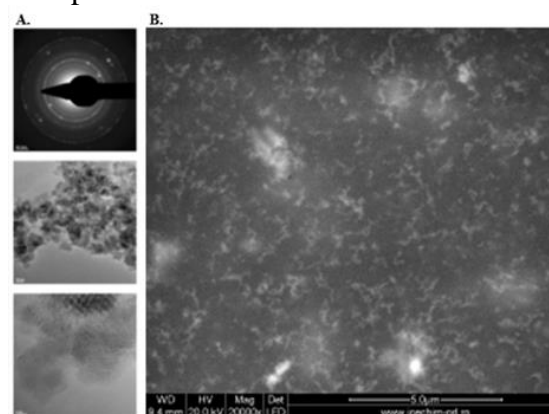


Fig. 5.9: TEM (A) and SEM (B) results for sample 5: (MNP + TMOH) + inulină + HA

### 5.2.2. Fourier Transform Infrared Spectroscopy (FT-IR) determinations

The FT-IR spectra of the experimental samples are shown in the following figures. All FT-IR spectra recorded between 400–4000  $\text{cm}^{-1}$  for experimental magnetic nanoparticles show the characteristic bands of ferroferric nanoparticles.

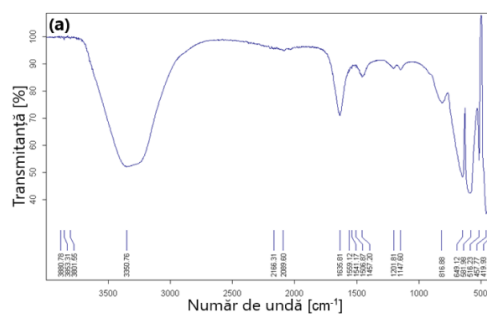


Fig. 5.10: FT-IR spectra for the experimental sample of synthesized MNPs

The spectrum recorded after the investigation of the experimental samples of magnetic nanoparticles (MNP) presented in figure 5.10, shows the wavelength band of  $581\text{ cm}^{-1}$  characteristic of magnetite ( $\text{Fe}_3\text{O}_4$ ). The band from wavelength of  $630\text{ cm}^{-1}$  is present in the spectra of all synthesized samples and demonstrates the presence of maghemite ( $\gamma\text{-Fe}_2\text{O}_3$ ). Hematite ( $\alpha\text{-Fe}_2\text{O}_3$ ) is also present in the analyzed ferrofluids, a fact demonstrated by the band from  $537\text{ cm}^{-1}$ .

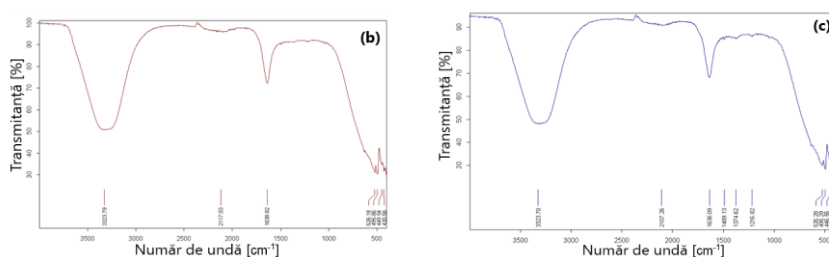


Fig. 5.11: FT-IR spectra for experimental samples: b) HA coated MNP; c) MNP coated with HA in increased concentration

In samples coated with hyaluronic acid in different concentrations (Figure 5.11), the broadband, from the wavelength of  $3330\text{ cm}^{-1}$  specific to the hydroxyl-OH group, moves to the right, to  $3340\text{ cm}^{-1}$  and  $3346\text{ cm}^{-1}$ , respectively, which demonstrates that a coating with hyaluronic acid took place.

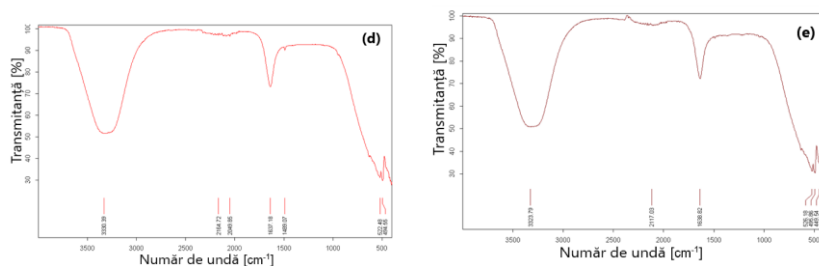


Fig. 5.12: FT-IR spectra for experimental samples: d) MNP with TMOH; e) MNP coated with TMOH and HA

FT-IR analysis of tetramethylammonium hydroxide (TMOH) coated ferrofluid shown in Figure 5.12 d) demonstrates the presence of the  $\text{-OH}$  group, due to the symmetrical and asymmetric stretching vibration that generates a wide band at  $3330\text{ cm}^{-1}$ . The intense band at  $1637\text{ cm}^{-1}$  can be designated both by the symmetrical stretching vibration from  $\text{-OH}$  in the  $\text{-COOH}$  group, and by the deformation vibration characteristic of the  $\text{C-N}$  group in TMOH.

The vibration from  $1489\text{ cm}^{-1}$  is given by the asymmetric stretch at  $\text{-C=O}$  in the  $\text{-COOH}$  group. In similar samples coated with hyaluronic acid (Figure 5.12 e)), the broadband, from the wavelength of  $3330\text{ cm}^{-1}$  specific to the hydroxyl-OH group moves to the right, at  $3340\text{ cm}^{-1}$  which proves that it occurred a coating with hyaluronic acid.

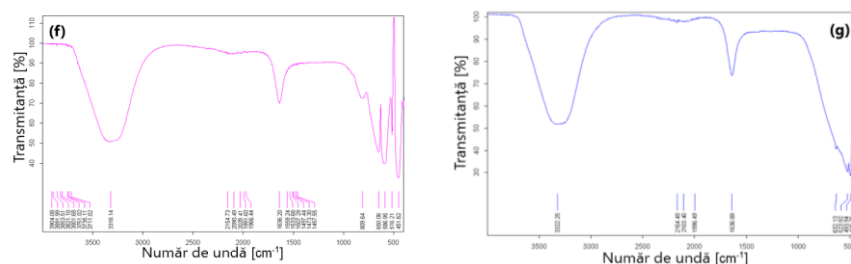


Fig. 5.13: FT-IR spectra for experimental samples: f) MNP with inulin; g) MNP coated with inulin and embedded in HA

The spectrum recorded after the investigation of the experimental samples of magnetic nanoparticles (MNP) presented in figure 5.10, shows band at the wavelength of  $581\text{ cm}^{-1}$  characteristic of magnetite ( $\text{Fe}_3\text{O}_4$ ). The  $630\text{ cm}^{-1}$  wavelength band is present in the spectra of all synthesized samples and demonstrates the presence of maghemite ( $\gamma\text{-Fe}_2\text{O}_3$ ). Hematite ( $\alpha\text{-Fe}_2\text{O}_3$ ) is also present in the analyzed ferrofluids, a fact demonstrated by the band from  $537\text{ cm}^{-1}$ .

### 5.2.3. Determination of nanoparticle sizes and zeta potential of experimental samples by DLS methods

The results of the experimental determinations are summarized in the following table.

Table 5.2: The size and value of the zeta potential of experimentally synthesized magnetic nanoparticles

Nr. crt.	Sample composition	DLS [nm]	Zeta potential [mV]
1	MPN	109,4	-44,6
2	MPN + HA	118	-67,7
3	MPN + TMOH	43,67	-42,4
4	MPN + TMOH + HA	101,6	-51,5
5	MPN + TMOH + inulină	50,14	-29,7
6	MPN + TMOH + inulină + HA	79,91	-42,4

The initial magnetic nanoparticles are in the form of agglomerations with dimensions around 100 nm, as can be seen in both Table 5.2 and Figure 5.14 a). The agglomerations deposit very quickly on the bottom of the container, which determined the stabilization of the magnetic nanoparticles by coating with a layer of TMOH (peptization), which leads to the destruction of the agglomerations.

After the addition of the TMOH layer, stable magnetic nanoparticles formed, which do not deposit over time (Figure 5.14 b)). The resulting dimensions were 43 nm, but the Zeta potential did not change obviously (Figure 5.15 b)).

The addition of the second layer, inulin, leads to an increase in particle size up to 50 nm, a rather insignificant increase given that the initial MNP agglomerations had 100 nm (Figure 5.14 d)).

After the deposition of the second coating (inulin), hyaluronic acid was added in two different concentrations, in a ratio of 1:10. In the two cases, magnetic nanoparticles with dimensions of 76 nm (Figure 5.14 e)) were obtained, respectively 243 nm for the concentration 10 times higher (Figure 5.14 c)). The Zeta potential does not change visibly, having the value of about -40 mV (Figure 5.15 c) and d)). It was observed that the sample with the lower HA concentration is more stable over time than the one with the high concentration, the smaller particle size being an important factor in favoring stability.

By comparing the data obtained, it was observed that, in the case of single-layer coated magnetic nanoparticles (MNP + TMOH), the addition of concentrated hyaluronic acid leads to biomaterials such as composite-biopolymer magnetic nanoparticles with relatively similar dimensions as for the use of magnetic nanoparticle coated with two layers (MNP + TMOH + Inulin).

This fact, corroborated with the values of the Zeta potential, demonstrates that in the case of the use of magnetic nanoparticles coated with two layers, the efficiency of dispersion in hyaluronic acid is similar.

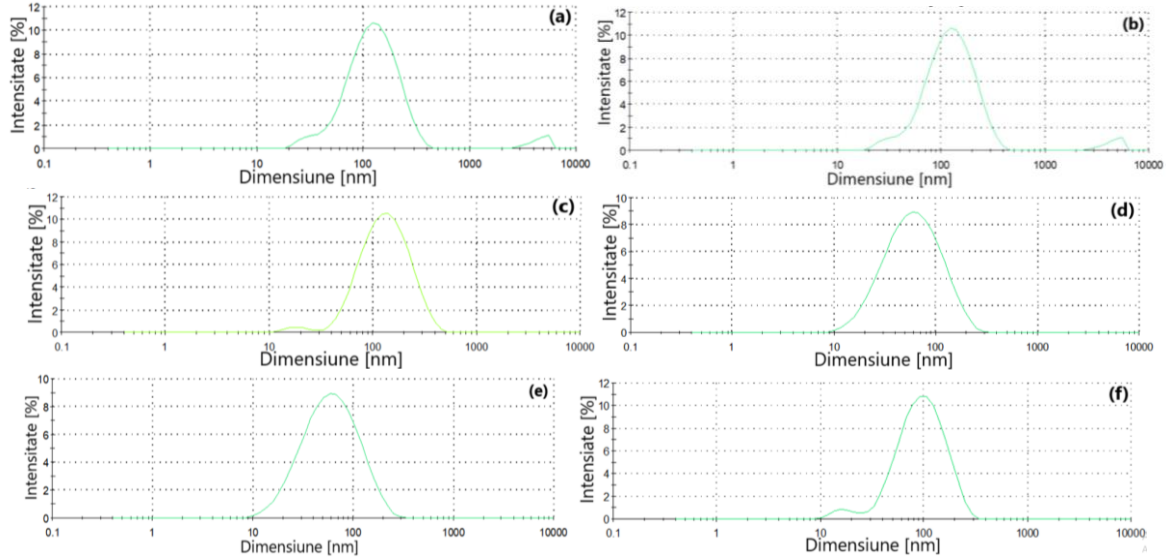


*Fig. 5.14: Distribution of nanoparticle size: a) Initial MNPs; b) MNPs coated with TMOH; c) MNPs coated with TMOH and concentrated HA; d) MNPs coated with TMOH and Inulin; e) MNPs coated with TMOH, Inulin and HA; f) MNPs coated with TMOH, Inulin and concentrated HA*

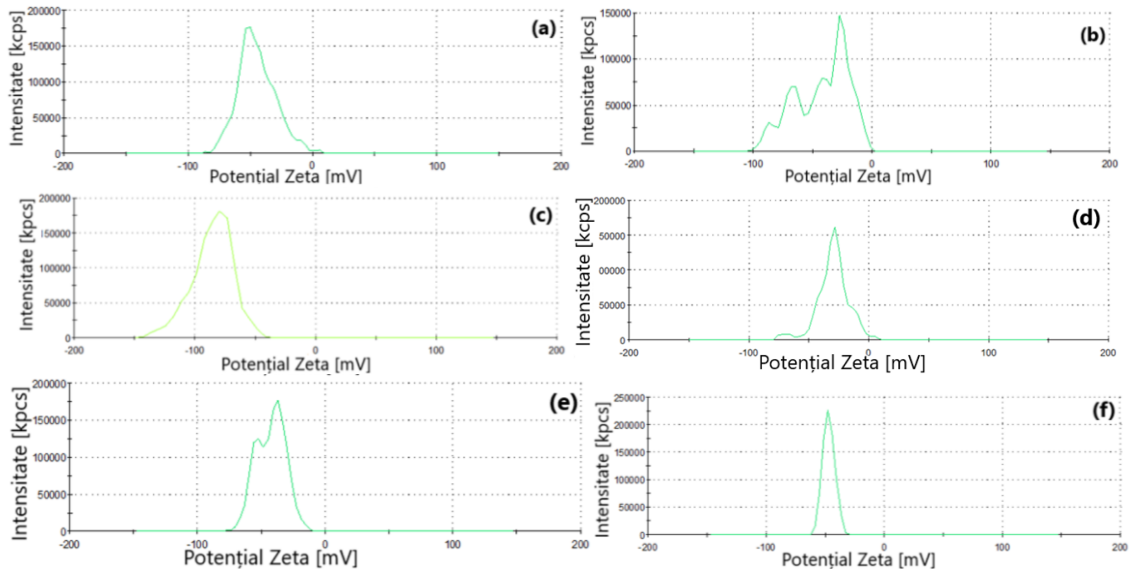


*Fig. 5.15: Distribution of the Zeta potential of nanoparticles: a) Initial MNPs; b) MNPs coated with TMOH; c) MNPs coated with TMOH and concentrated HA; d) MNPs coated with TMOH and Inulin; e) MNPs coated with TMOH, Inulin and HA; f) MNPs coated with TMOH, Inulin and concentrated HA*

## CHAPTER 6: TESTING OF VISCOELASTIC SOLUTIONS

### 6.1. Rheological testing of improved viscoelastic solutions with drug-carrying magnetic nanoparticles

Rheological tests performed on classical viscoelastic solutions highlight the fact that they are slightly sensitive to contact with air and slightly change their rheological properties over time (due to the hysteresis that occurs on the return curve). This is normal, due to the structural changes and the properties of hyaluronic acid in the composition of the viscoelastic solution. Both the elastic modulus and the viscous modulus vary over time and stabilize around the values of  $G' = 150\text{Pa}$  and  $G'' = 400\text{Pa}$ , results in accordance with the data in the literature and those provided by the manufacturers.

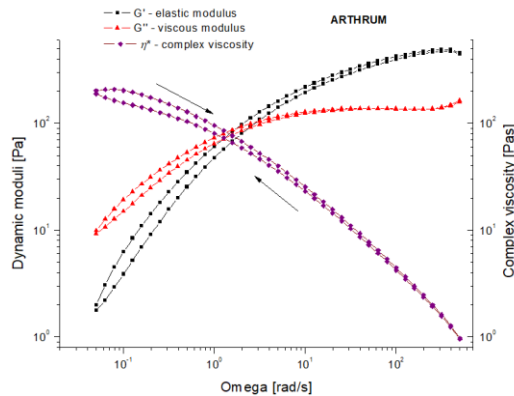


Fig 6.1: Rheological test results for the ARTHRUM solution, considered as reference

The introduction of magnetic nanoparticles into the viscoelastic solution slightly reduces the viscosity of the initial solutions. From a rheological point of view, it generally varies linearly with the concentration of nanoparticles used.

A complex rheological analysis of three types of viscous supplement solutions (Artrum-A, Neovisc-N and Jointex-J) modified with magnetic nanoparticles was also performed. It is observed that the Artrum solution has better viscosity properties, probably due to the fact that it has a higher concentration of hyaluronic acid in the composition.

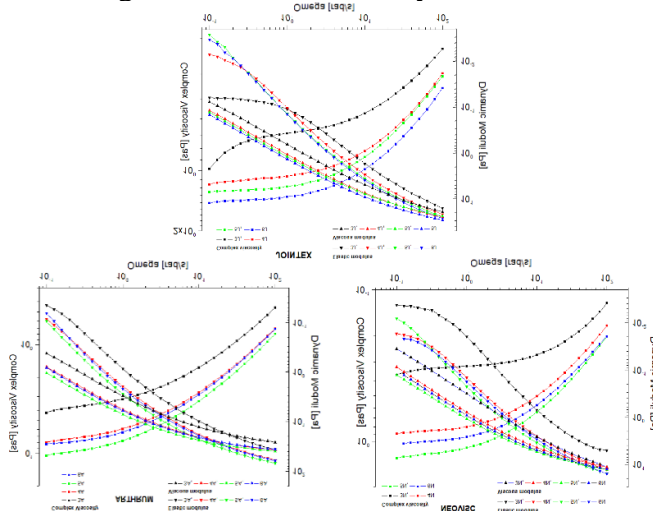


Fig. 6.2: Results of rheological tests for commercial viscoelastic solutions modified with magnetic nanoparticles

The final experimental samples of nanoparticles (table 6.1.) will be introduced into the viscoelastic solution with a concentration of 32 mg / 2ml and characterized

experimentally. For a better evaluation, the solution of magnetic nanoparticles was diluted in different concentrations (the synthesis concentration was diluted 10, 50 and 100 times compared to the synthesis solution).

Table 6.1: Composition of viscoelastic solutions prepared for rheology tests

Sample	Composition	Sample code (for rheology tests)
1	MNP+ HA	3N
2	(MNP + TMOH) + HA	3J
3	((MNP + TMOH) + inulină + HA	3A
4	MNP /10 + HA	4N
5	(MNP + TMOH)/10 + HA	4J
6	((MNP + TMOH)/10 + inulină + HA	4A
7	MNP /50 + HA	5N
8	(MNP + TMOH)/50 + HA	5J
9	((MNP + TMOH)/50 + inulin + HA	5A
10	MNP /100 + HA	6N
11	(MNP + TMOH)/100 + HA	6J
12	((MNP + TMOH)/100 + inulin + HA	6A

The magnetic nanoparticles were initially diluted to the desired concentrations, then peptized with TMOH, and coated with inulin, respectively. All samples were functionalized with hyaluronic acid, in a volumetric ratio of 1:1. The experimental results are presented in the following figures.

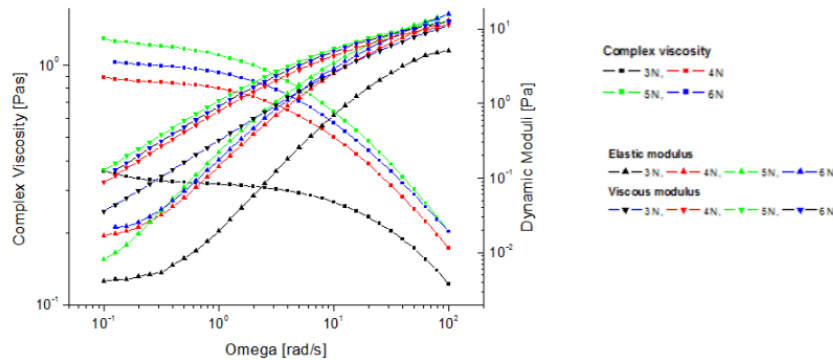


Fig. 6.3: Results of rheological tests for improved viscoelastic solutions with magnetic nanoparticles type (MNP HA), in different concentrations: 3N; 4N; 5N; 6N

Compared to the results obtained for the viscoelastic solution without magnetic nanoparticles (Figure 6.1), The graphs for the samples in which a certain concentration of MNP was added show that by introducing them the viscosity of the initial solutions is slightly reduced.

Taking into account the concentration of nanoparticles used, from a rheological point of view it can be said that the properties of nanoparticles vary, depending on the dilution rate, the best properties having the solutions diluted 50 and 100 times compared to the initial concentration. Also, the best results are those obtained for nanoparticles peptized with TMOH and coated with HA - concentrations diluted 100 and 50 times, respectively those peptized with TMOH and coated with HA - concentrations diluted 100 and 50 times.

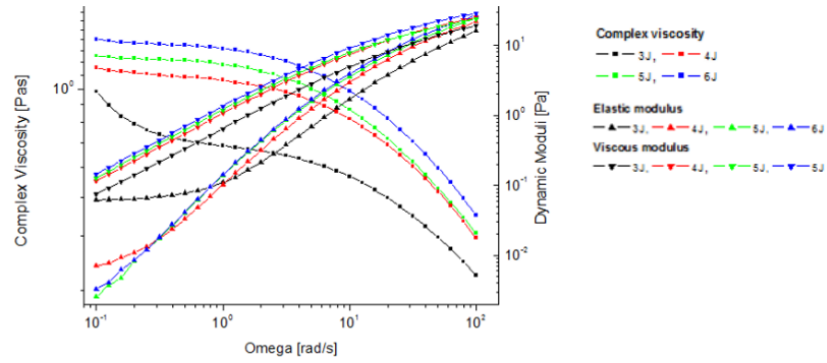


Fig. 6.4: Results of rheological tests for viscoelastic solutions improved with magnetic nanoparticles of the type (MNP + TMOH) + HA, in different concentrations: 3J; 4J; 5J; 6J

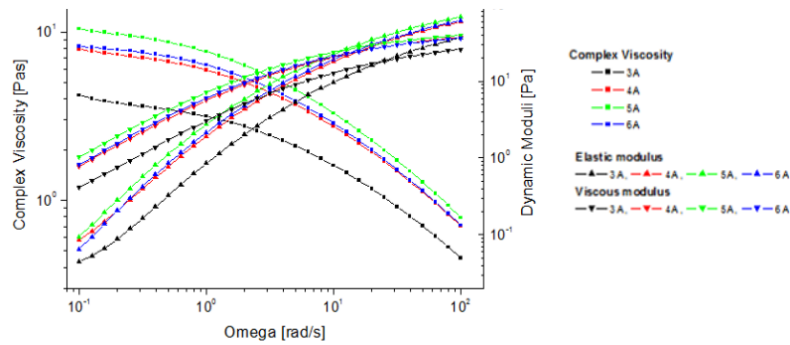


Fig. 6.5: Results of rheological tests for improved viscoelastic solutions with magnetic nanoparticles of the type ((MNP + TMOH) + inulin) + HA, in different concentrations: 3A; 4A; 5A; 6A

The results of rheological tests performed suggest that magnetic nanoparticles such as (MNP + TMOH) + HA and ((MNP + TMOH) + inulin) + HA, in which MNP have been diluted 50 and 100 times are optimal. It was also pointed out that the undiluted solutions had the worst results for each type of sample and therefore these samples were further abandoned.

In order to highlight the positive influence of the magnetic field exerted by permanent magnets used clinically in combination with viscoelastic solutions enhanced with MNP, rheological tests were performed in the magnetic field.

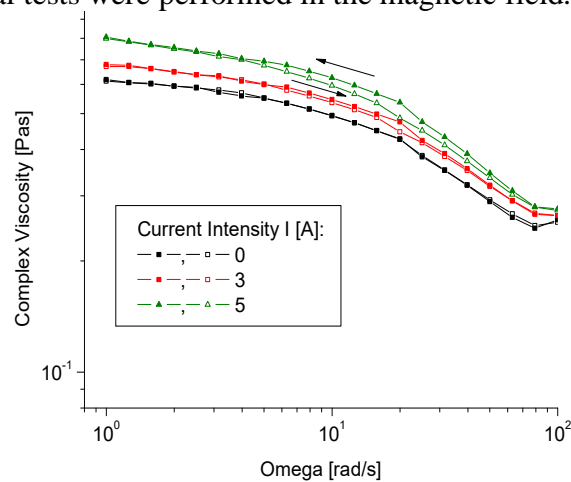


Fig. 6.6: Result of rheology tests under the influence of the magnetic field for the improved viscoelastic solution with magnetic nanoparticles ((MNP + TMOH) / 50 + inulin) + HA

The sample ((MNP + TMOH)/50 + inulin) + HA, showed the best results (Figure 6.6). It is highlighted that there is a more stable behavior of the solutions after they have been exposed to a magnetic field (the hysteresis for the "return path" is significantly reduced). This confirms the usefulness and efficiency of the proposed solution to use permanent magnets in the composition of the orthosis associated with the viscoelastic solution enhanced with nanoparticles used in the treatment of knee disorders.

## 6.2. Testing the magnetic properties of improved viscoelastic solutions with drug-carrying magnetic nanoparticles

### 6.2.1. Using the COMSOL modeling program

During the experiment, several magnet configurations were observed in which the volume and distances between them vary. The following figure (Fig. 6.4) shows the geometries used in the two optimization processes.

Two approaches to solving this problem have been considered.

A. The first method was based on the use of an area of 0.01 m, as a reference, in which the magnets were placed. In this case it is a simple division of the first magnet with the dimensions of 0.01x0.002 m into matrices of 2, 3, respectively 4 magnets. Using this approach, the properties of the magnets are manipulated by reducing the surface, as well as the total energy of the magnets. The division conditions of the magnets are illustrated, observing a division of the permanent magnets according to the gradient of the ratio  $d_1/d_2$ , where  $d_1$  represents the length of a magnet, and  $d_2$  the distance between the magnets. Thus the geometries can be divided for each type of matrix separately in three other cases correlated with the values of the ratio  $d_1/d_2$ , namely:

- 1) Case I:  $d_1/d_2 < 1$ ;
- 2) Case II:  $d_1/d_2 = 1$ ;
- 3) Case III:  $d_1/d_2 > 1$ .

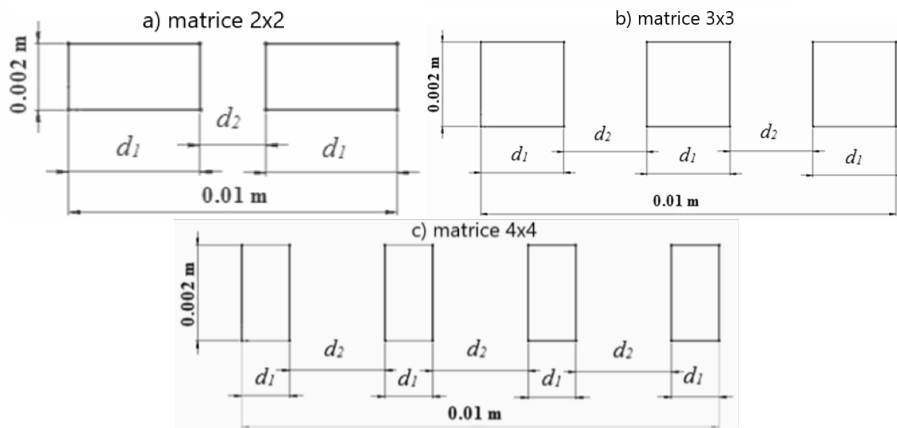


Fig. 6.7: Magnet matrix for 2D models: a) 2 magnets; b) 3 magnets; c) 4 magnets

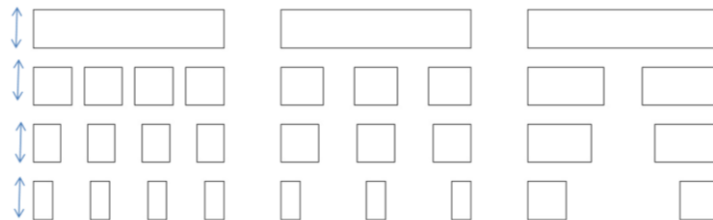
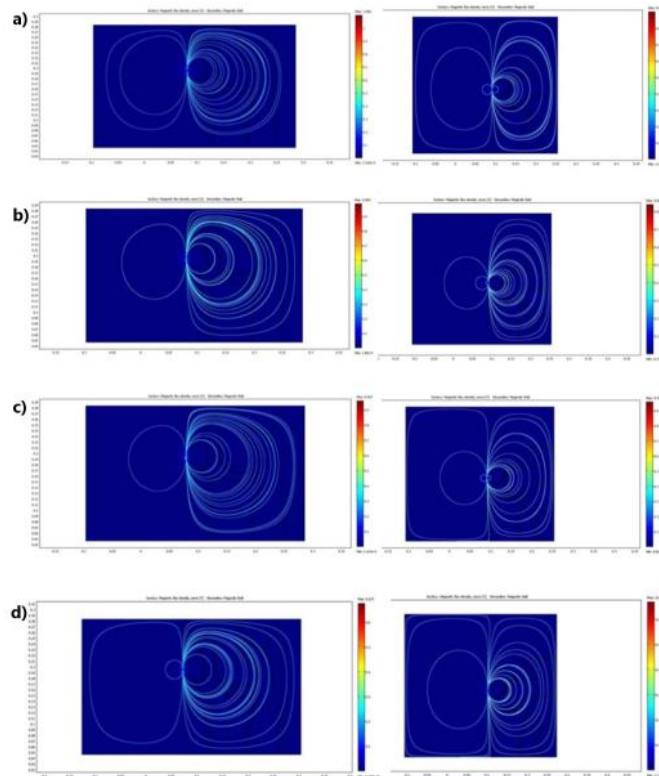


Fig. 6.8: COMSOL geometries for the first simulation model

In the figure above (Fig. 6.8) we have the different geometries divided into cases, taking into account both the number of magnets and the distances between them, used in modeling. These conditions bring to our attention a number of 9 cases. The situation of existence of a single magnet will also be analyzed, in order to be able to make case comparisons. Following the case modeling, different magnetic fields are obtained.

The most important movements of the knee are flexion and extension, to which the associated movements in plane, rotation and translation are coupled. Therefore, this study will consider the two extreme positions of the knee, namely the  $0^\circ$  position and the  $90^\circ$  position.

In order to analyze the different magnet positioning situations, the forces that appear behind the kneecap shall be measured. These forces are measured in  $[\text{N}/\text{m}^3]$  and evaluate the volumic force as described by the Navier-Stokes equations implemented in COMSOL in the Fluid Dynamics module. This can be expressed as a pressure reported to the unit of length  $[\text{N}/\text{m}^2 = \text{Pa}] / [\text{m}] = [\text{N}/\text{m}^3]$ .



*Fig. 6.9: COMSOL modeling for the two reference positions:  $0^\circ$  (left) and  $90^\circ$  (right) illustrating the induction and magnetic field for the cases: a) One magnet, b) Two magnets measuring  $0.004 \times 0.002 \text{m}$  ( $d_1/d_2 < 1$ ), c) Two magnets with dimensions  $0.0034 \times 0.002 \text{m}$  ( $d_1/d_2 = 1$ ), d) Two magnets with dimensions  $0.002 \times 0.002 \text{m}$  ( $d_1/d_2 > 1$ )*

Figure 6.9 illustrates two components that characterize magnets, namely the density of magnetic flux and the field lines generated for the existence of a single magnet and the three cases of the existence of a matrix of two magnets positioned more and more distant. It is noted that the greater the distance between the magnets, the lower the forces on the Ox axis, but also those on the Oy axis, the ferrofluid having the tendency to move under normal conditions without encountering opposing forces. As seen in Figure 6.10, the magnitude of the magnetic field generated by a matrix of two magnets decreases from case b) to case d).

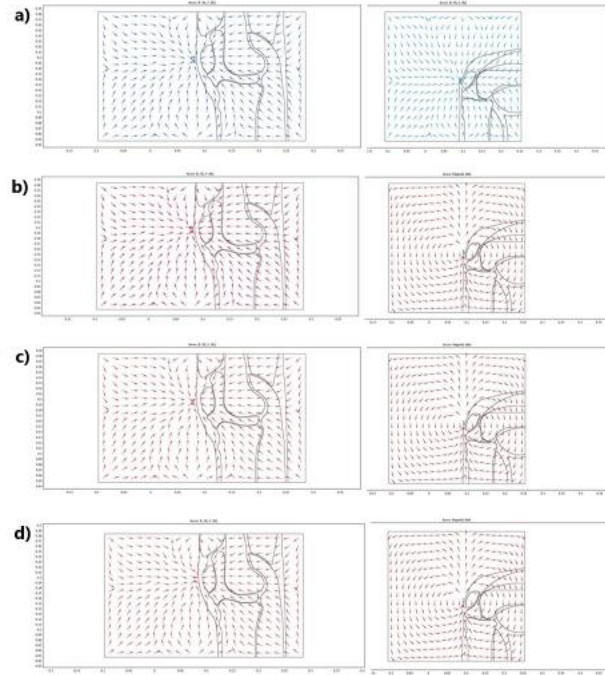


Fig. 6.10: COMSOL modeling for the two reference positions:  $0^\circ$  (left) and  $90^\circ$  (right) illustrating by means of the arrows the directions on the X and Y axis of the knee magnetization for the cases: a) One magnet, b) Two magnets with dimensions  $0.004 \times 0.002 \text{ m}$  ( $d1/d2 < 1$ ), c) Two magnets with dimensions  $0.0034 \times 0.002 \text{ m}$  ( $d1/d2 = 1$ ), d) Two magnets with dimensions  $0.002 \times 0.002 \text{ m}$  ( $d1/d2 > 1$ )

The magnet with a side of 0.002 and a height of 0.01m (Figure 6.9 a)) will represent the reference magnet. The following models will be based on the shape of this magnet divided into matrices of two, three and four magnets on a 2D model.

The value of the remaining induction reaches 1,218517 [T], in the area of the ferrofluid location and influences it by means of two components one in the direction of the  $O_x - F_x$  axis, and one in the direction of  $O_y - F_y$ . In this first case  $F_x = -4.20776 \text{ [N/m}^3]$  and  $F_y = 0.371098 \text{ [N/m}^3]$ .

For the  $0^\circ$  position of the knee the force values are  $F_x = -4.211314 \text{ [N/m}^3]$ , and  $F_y = 1.13 \text{ [N/m}^3]$  respectively. Based on these values we can conclude that the movement of the knee from one position to another brings changes in the magnetic field predominantly in the direction of  $O_y$ , in order to draw the ferrofluid mass upwards, towards the back of the kneecap. This trend is favorable to us, as the  $F_y$  force opposes the relocation of the ferrofluid behind the patello-femoral zone.

The magnet exerts a magnetic induction on the kneecap of 1.226259 [T], while the target area feels a lower value, 1.218517 [T]. Figure 6.10 illustrates the orientation of the forces acting in each case. The arrows show the mode of movement that will be followed by the ferrofluid placed in the intra-articular space.

On a case-by-case basis, decreases of approximately  $1 \text{ N/m}^3$  are observed as the distance  $d2$  increases in relation to  $d1$  in the case of the 2x2 matrix.

Following the same simulation procedure, the following cases 3x3 (Figures 6.11 and 6.12) and 4x4 (Figures 6.13 and 6.14) presented below will show the same trend of displacement of the ferrofluid, drawn horizontally by the  $F_x$  force to the magnets and raised to the kneecap by  $F_y$  force.

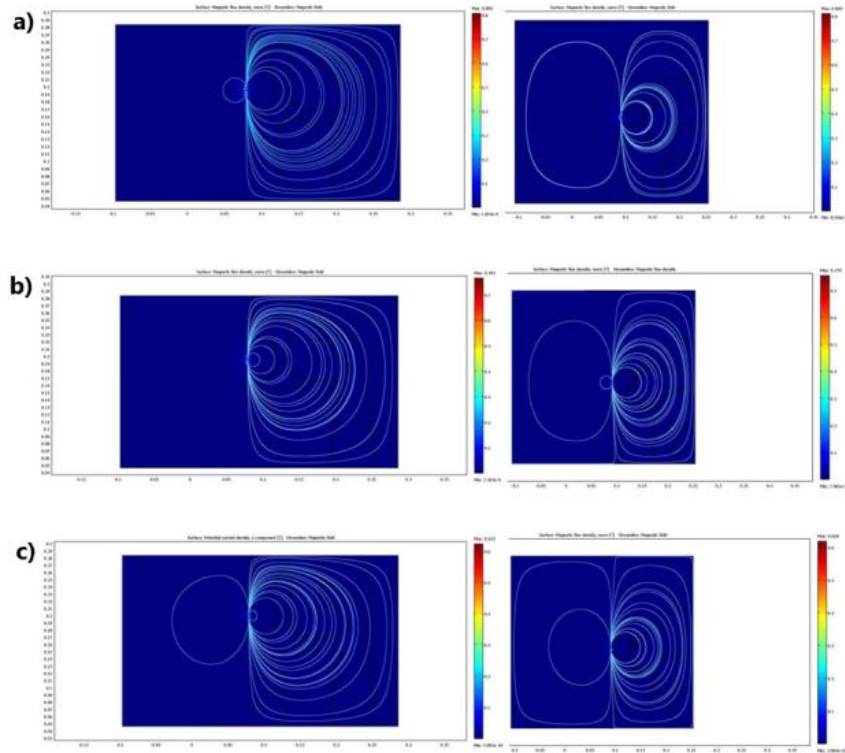


Fig. 6.11: Comsol modeling for the two reference positions:  $0^\circ$  (left) and  $90^\circ$  (right) illustrating the induction and magnetic field for the cases: a) Three magnets with dimensions:  $0.00225 \times 0.002 \text{m}$  ( $d_1/d_2 < 1$ ), b) Three magnets measuring  $0.002 \times 0.002 \text{m}$  ( $d_1/d_2 = 1$ ), c) Three magnets with dimensions  $0.001 \times 0.002 \text{m}$  ( $d_1/d_2 > 1$ )

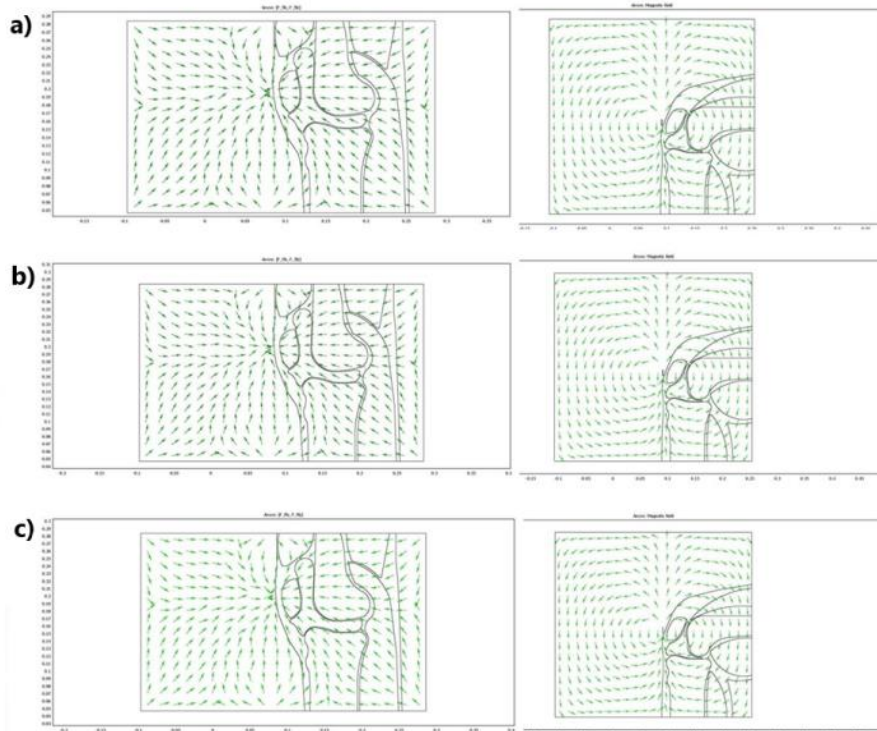


Fig. 6.12: Comsol modeling for the two reference positions:  $0^\circ$  (left) and  $90^\circ$  (right) by means of arrows the directions on the X and Y axis of the magnetization for the cases: for the cases: a) Three magnets with dimensions:  $0.00225 \times 0.002 \text{m}$  ( $d_1/d_2 < 1$ ), b) Three magnets with dimensions  $0.002 \times 0.002 \text{m}$  ( $d_2/d_2 = 1$ ), c) Three magnets with dimensions  $0.001 \times 0.002 \text{m}$  ( $d_1/d_2 > 1$ )

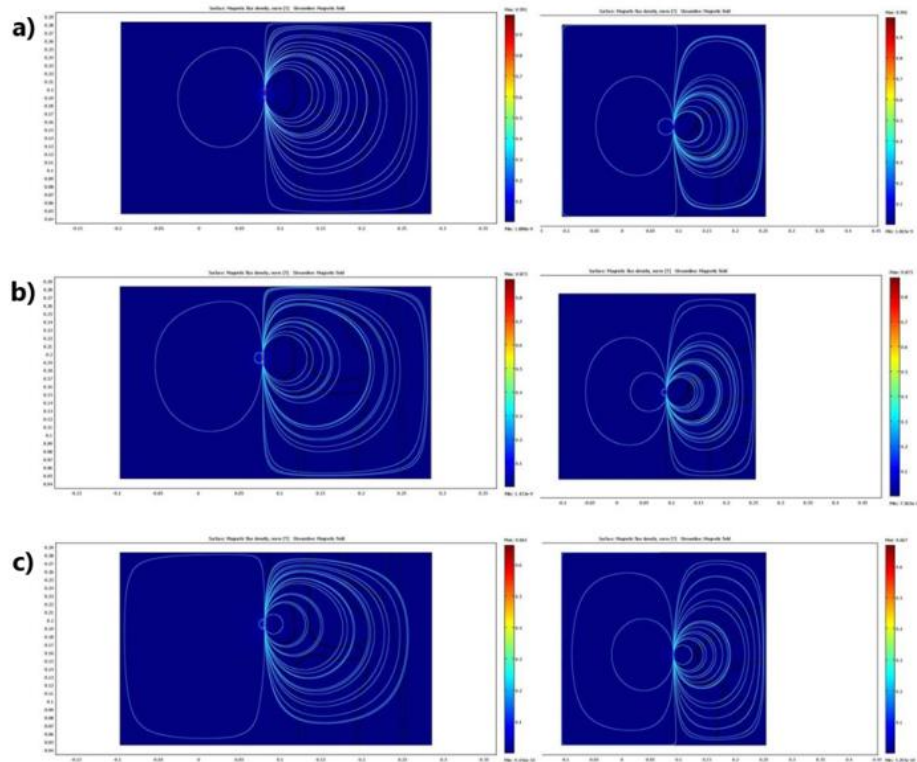


Fig. 6.13: Comsol modeling for the two reference positions:  $0^\circ$  (left) and  $90^\circ$  (right) illustrating the induction and magnetic field for the cases: a) Four magnets with dimensions  $0.002 \times 0.002 \text{ m}$  ( $d_1/d_2 < 1$ ), b) Four magnets with the dimensions  $0.001429 \times 0.002 \text{ m}$  ( $d_1/d_2 = 1$ ), c) Four magnets with dimensions  $0.001 \times 0.002 \text{ m}$  ( $d_1/d_2 > 1$ )

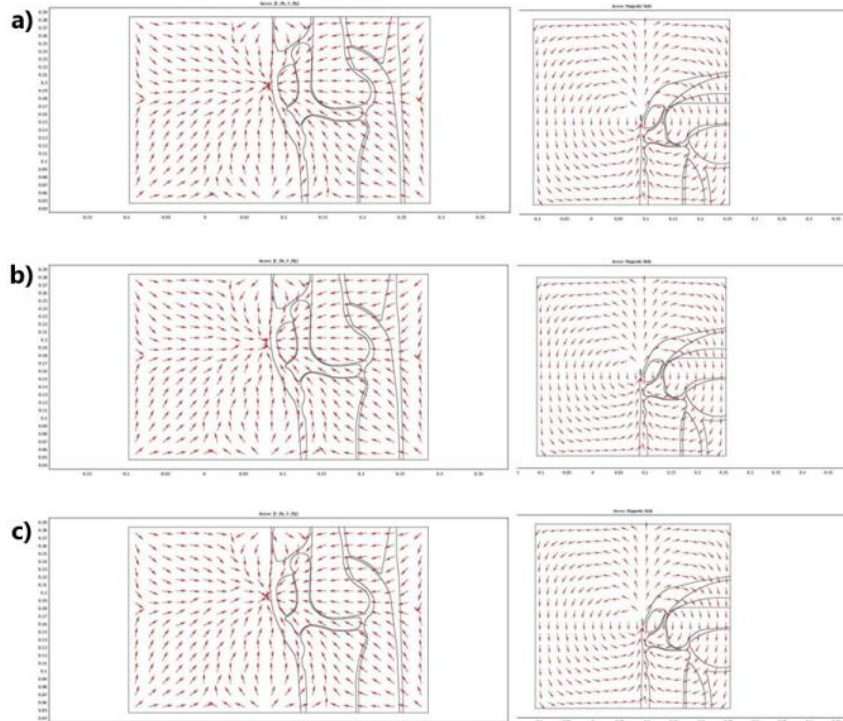


Fig. 6.14: Comsol modeling for the two reference positions:  $0^\circ$  (left) and  $90^\circ$  (right) illustrating by means of the arrows the directions on the X and Y axis of magnetization for the cases: a) Four magnets with dimensions  $0.002 \times 0.002 \text{ m}$  ( $d_1/d_2 < 1$ ), b) Four magnets with dimensions  $0.001429 \times 0.002 \text{ m}$  ( $d_1/d_2 = 1$ ), c) Four magnets with dimensions  $0.001 \times 0.002 \text{ m}$  ( $d_1/d_2 > 1$ )

Tabel 6.2: The values of the volumic forces generated following the modeling in COMSOL of the 9 cases of configuration of the magnets for the knee joint at 0°

Forces	Conditions	2 magnets	3 magnets	4 magnets	1 magnet 0.01x0.04	1 magnet 0.002x0.01
F_ffx[N/m <sup>3</sup> ]	Case I: d <sub>1</sub> /d <sub>2</sub> <1	-2.677207	-1.544629	-2.686054	-675.868462	-4.20776
	Case II: d <sub>1</sub> /d <sub>2</sub> =1	-1.500033	-1.218848	-1.107127		
	Case III: d <sub>1</sub> /d <sub>2</sub> >1	-0.605071	-0.298958	-0.667311		
F_ffy[N/m <sup>3</sup> ]	Case I: d <sub>1</sub> /d <sub>2</sub> <1	0.23623	0.132684	0.237069	79.579543	0.371098
	Case II: d <sub>1</sub> /d <sub>2</sub> =1	0.128839	0.105626	0.095158		
	Case III: d <sub>1</sub> /d <sub>2</sub> >1	0.053892	0.025224	0.058891		

Tabel 6.3: The values of the volumic forces generated following the modeling in COMSOL of the 9 cases of configuration of the magnets for the knee joint at 90°

Forces	Conditions	2 magnets	3 magnets	4 magnets	1 magnet 0.01x0.04	1 magnet 0.002x0.01
F_ffx[N/m <sup>3</sup> ]	Case I: d <sub>1</sub> /d <sub>2</sub> <1	-4.040907	-2.830486	-4.058452	-318.605131	-4.211314
	Case II: d <sub>1</sub> /d <sub>2</sub> =1	-2.74248	-2.266462	-2.03011		
	Case III: d <sub>1</sub> /d <sub>2</sub> >1	-0.984864	-0.551917	-0.990473		
F_ffy[N/m <sup>3</sup> ]	Case I: d <sub>1</sub> /d <sub>2</sub> <1	1.089556	0.751898	1.09923	67.541691	1.130408
	Case II: d <sub>1</sub> /d <sub>2</sub> =1	0.721633	0.609243	0.539532		
	Case III: d <sub>1</sub> /d <sub>2</sub> >1	0.2575	0.144148	0.261463		

Using the data in tables 6.2 and 6.3, the graphs in figures 6.15 and 6.16 can be showed the influence of parameter d2 on field intensity.

According to the performances in the graphs shown below, one can observe the uneven behavior of magnets positioned in 4x4 matrices. This inflection of the curve determines that the 4x4 matrix has the best behavior and is therefore the best choice for joint applications. A similarity can be observed between the 2 magnet matrices and the 4 magnet matrices, but this applies only to the first case of the d<sub>1</sub>/d<sub>2</sub> ratio. The curve corresponding to the 2x2 matrix shows a linear evolution which is unfavourable for the drug delivery systems.

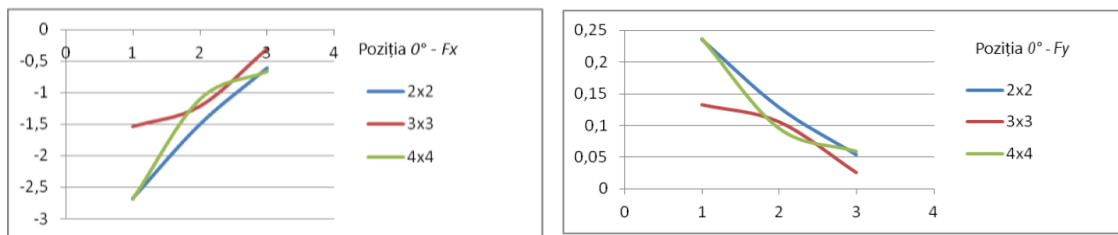


Fig. 6.15: Representation of the 3 curves given by the volumic forces in the directions: left - Ox, applied on the model of the joint positioned at an angle of 0°, which tend to attract ferrofluid to the magnets and right - OY, applied on the model of the joint positioned at an angle of 0°, which tend to resist the slip of ferrofluid under the pressure forces existing in the joint

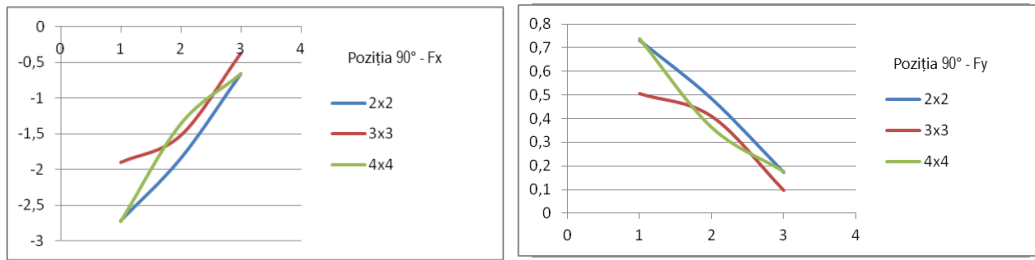


Fig. 6.16: Representation of the 3 curves given by the volumic forces in the directions: left -  $Ox$ , applied to the model of the joint positioned at  $90^\circ$  angle, which tend to attract the ferrofluid to the magnets and down -  $OY$ , applied to the model of the joint positioned at a  $90^\circ$  angle, which tend to resist the slip of the ferrofluid under the pressure forces existing in the joint

**B.** The second part of the modelling takes into account an action area 10 times larger than the previous one, based on the justification that an surface covering the entire area of interest would be more effective. Thus we obtained a number of 18 cumulative cases for extreme positions. The geometries concerned shall consider modifying the two dimensions of the magnets, but keeping the same energy throughout the system. The volume of components will be the common denominator in all.

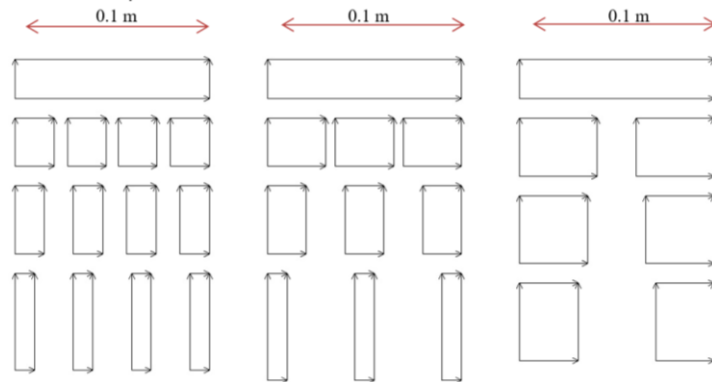


Fig. 6.17: COMSOL geometries for the second simulation model

Similarly, the previous optimization, the magnet positioning mode related to the  $d1/d2$  ratio gradient will be retained.

In this second simulation study the size of magnets is reflected in the volumic forces they generate. For the first case of the matrix of 2 magnets,  $F_x = -5787.15 \text{ N/m}^3$ , a value 5000 times higher than in the first simulation study. It is considered that in the first simulations the division of magnets also had the consequence of a decrease in the total energy in the system. As in previous cases, with the increase in the distance between magnets decreases the volumic force on the  $Ox$  axis which is intended to attract particles. This is also based on the fact that these magnets the closer they are to the more uniform they behave by tending to form a single magnet.

The following figures show the density of magnetic flux for the same cases presented above, adapted to the geometry configuration corresponding to the second optimisation process, namely:

- Two magnets with dimensions: a)  $0.04 \times 0.03\text{m}$ , b)  $0.035 \times 0.035\text{m}$ , c)  $0.03 \times 0.04\text{m}$  (Fig. 6.18);
- Three magnets with dimensions: a)  $0.03 \times 0.025\text{m}$ , b)  $0.02 \times 0.035\text{m}$ , c)  $0.01 \times 0.055\text{m}$  (Fig. 6.19);
- Four magnets with dimensions: a)  $0.02 \times 0.025\text{m}$ , b)  $0.015 \times 0.035\text{m}$ , c)  $0.01 \times 0.05\text{m}$  (Fig. 6.20).

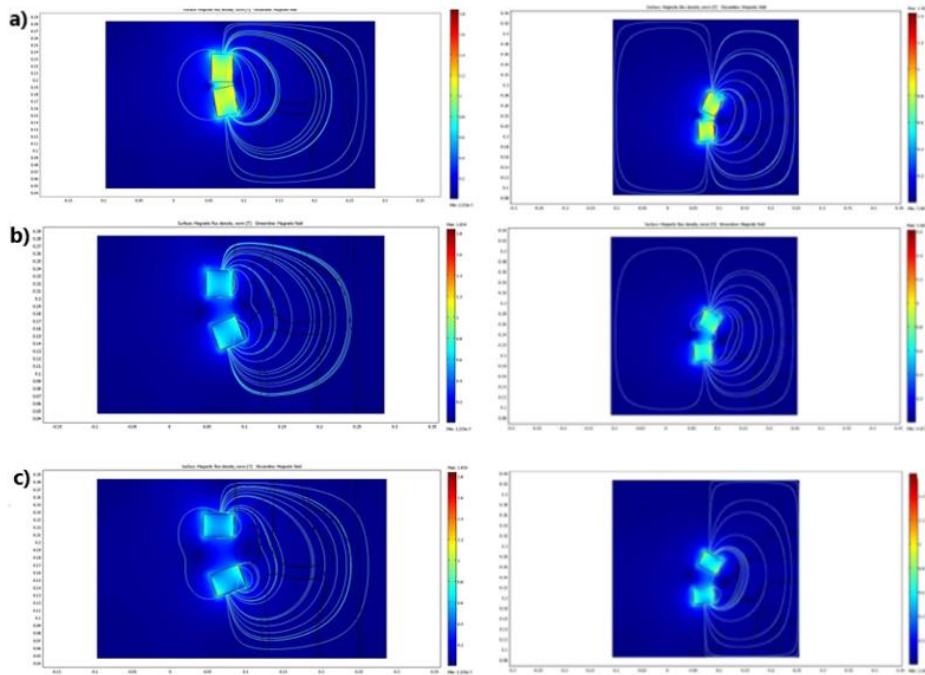


Fig. 6.18: COMSOL modeling for the two reference positions:  $0^\circ$  (left) and  $90^\circ$  (right) illustrating induction and magnetic field when using two magnets with dimensions: a)  $0.04 \times 0.03\text{m}$  ( $d_2/d_2 < 1$ ),  $0.035 \times 0.035\text{m}$  ( $d_1/d_2 = 1$ ), c)  $0.03 \times 0.04\text{m}$  ( $d_2/d_2 > 1$ )

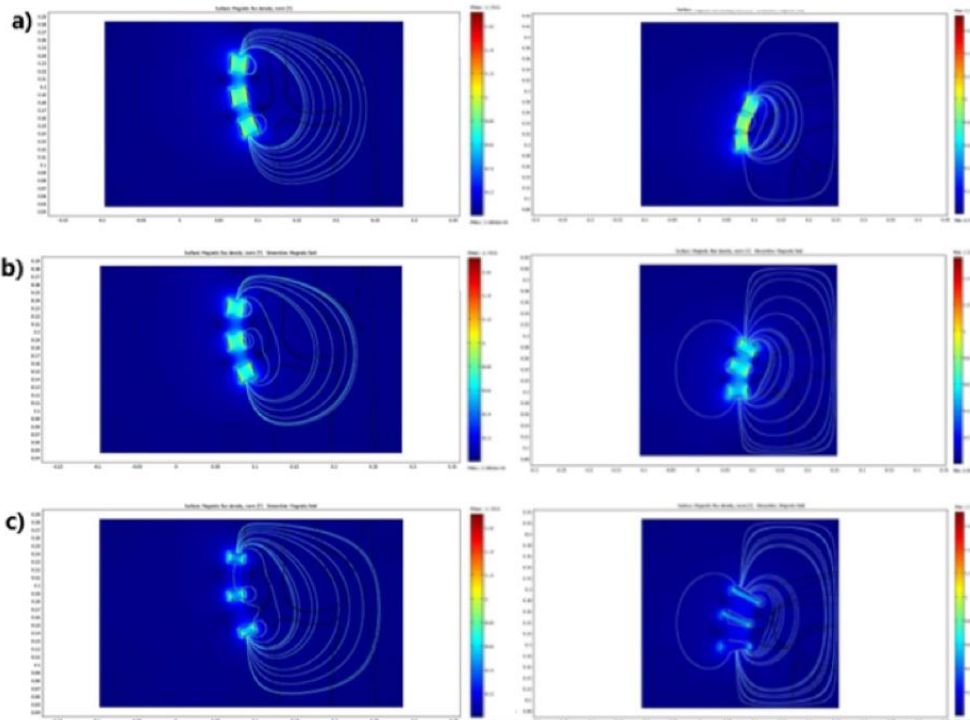


Fig. 6.19: COMSOL modeling for the two reference positions:  $0^\circ$  (left) and  $90^\circ$  (right) illustrating induction and magnetic field when using three magnets with dimensions: a)  $0.03 \times 0.025\text{m}$  ( $d_2/d_2 < 1$ ),  $0.02 \times 0.035\text{m}$  ( $d_1/d_2 = 1$ ), c)  $0.01 \times 0.055\text{m}$  ( $d_1/d_2 > 1$ )

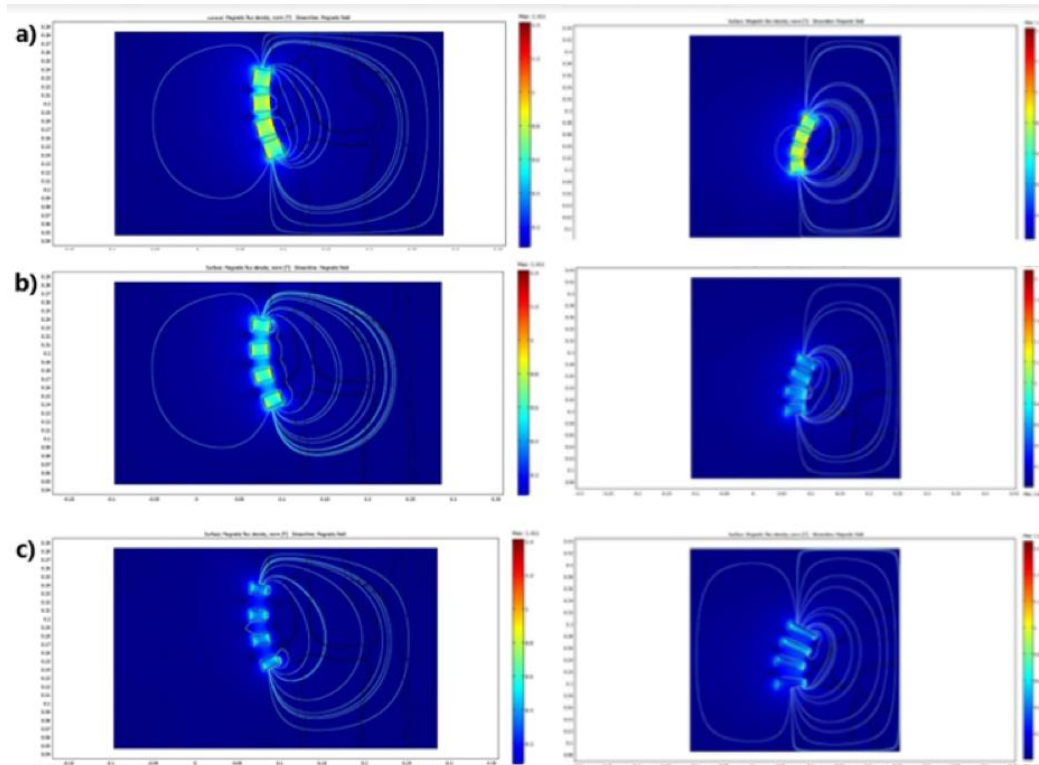


Fig. 6.20: COMSOL modeling for the two reference positions: 0° (left) and 90° (right) illustrating the induction and magnetic field when using four magnets with dimensions: a) 0.02x0.025m ( $d1/d2 < 1$ ), b) 0.015x0.035m ( $d1/d2 = 1$ ), c) 0.01x0.05m ( $d1/d2 > 1$ )

According to the previous figures, we can observe using the identifying colors of the magnetic flux density, a yellow coloration for case a), which suggest the presence of a magnetic field with induction close to 1.2 T. In cases b) and c) the interactions between magnets cause a decrease in their attraction power.

An undesirable effect that occurs in the cases presented is the behavior of the volumic force in the direction of  $O_y$ , which recording only high negative values tends to move the mass of nanoparticles in the direction of the force of gravity, opposite our objectives.

In order to have the best results in the drugs delivery in the patella-femoral target area, according to the results obtained after the mathematical modelling of the magnets, we can conclude that a matrix consisting of 4 lines of 4 magnets that can be fixed near the kneecap, at the distances related to the ratio:  $d1/d2 < 1$ , in order to have the greatest concentration of magnetic nanoparticles functionalized near the kneecap.

In tables 6.4 and 6.5 the values of the volumic forces for each direction,  $O_x$  and  $O_y$ , are presented in each case studied and for each position of the knee respectively.  $F_y$  volumic force values, according to Table 6.4, are predominantly negative, with the case of positioning four magnets on the same line being the only variant that exhibits optimal behavior of all three magnet choice options.

This conclusion is also attested by the values obtained for mathematical modeling in the flexion position, at an angle of 90°, of the knee joint, where, although the variant of choosing a matrix with two magnets generates the strongest magnetic field, the variant shown in Figure 6.21 - left is supported by the results of the 0° simulation of the knee joint, shown in Figure 6.17.

Tabel 6.4: The values of the volumic forces generated following the modeling in COMSOL of the 9 cases of configuration of the magnets for the knee joint at 0°

Forces	Conditions	2 magnets	3 magnets	4 magnets
F_ffx[N/m <sup>3</sup> ]	Case I: d <sub>1</sub> /d <sub>2</sub> <1	-5787.148562	-52.804538	-769.02699
	Case II: d <sub>1</sub> /d <sub>2</sub> =1	-2812.83292	27.980095	-238.696417
	Case III: d <sub>1</sub> /d <sub>2</sub> >1	-2553.342974	-26.418441	-51.826946
F_ffy[N/m <sup>3</sup> ]	Case I: d <sub>1</sub> /d <sub>2</sub> <1	-816.07387	-249.575446	-234.165625
	Case II: d <sub>1</sub> /d <sub>2</sub> =1	-1764.591395	-159.027015	218.835868
	Case III: d <sub>1</sub> /d <sub>2</sub> >1	-1707.281901	39.54396	58.474645

Tabel 6.5: The values of the volumic forces generated following the modeling in COMSOL of the 9 cases of configuration of the magnets for the knee joint at 90°

Forces	Conditions	2 magnets	3 magnets	4 magnets
F_ffx[N/m <sup>3</sup> ]	Case I: d <sub>1</sub> /d <sub>2</sub> <1	-1837.395508	-1547.774242	-1387.155461
	Case II: d <sub>1</sub> /d <sub>2</sub> =1	-1223.25802	-821.797657	-1113.182765
	Case III: d <sub>1</sub> /d <sub>2</sub> >1	-796.643546	-172.381984	-680.469698
F_ffy[N/m <sup>3</sup> ]	Case I: d <sub>1</sub> /d <sub>2</sub> <1	1422.907126	951.632468	583.505956
	Case II: d <sub>1</sub> /d <sub>2</sub> =1	1710.927069	880.339808	789.183377
	Case III: d <sub>1</sub> /d <sub>2</sub> >1	1647.965021	223.488876	471.026188

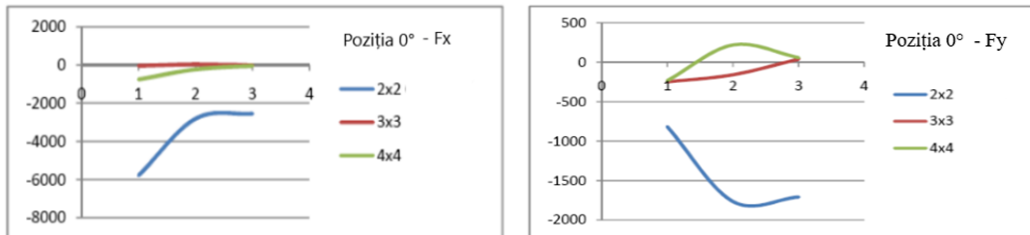


Fig. 6.21: Representation of the 3 curves given by the volumic forces: left - in the Ox direction, applied on the model of the joint positioned at an angle of 0°, which tend to attract ferrofluid to the magnets and right - in the Oy direction, which tend to resist slipping ferrofluid under the pressure forces existing in the joint

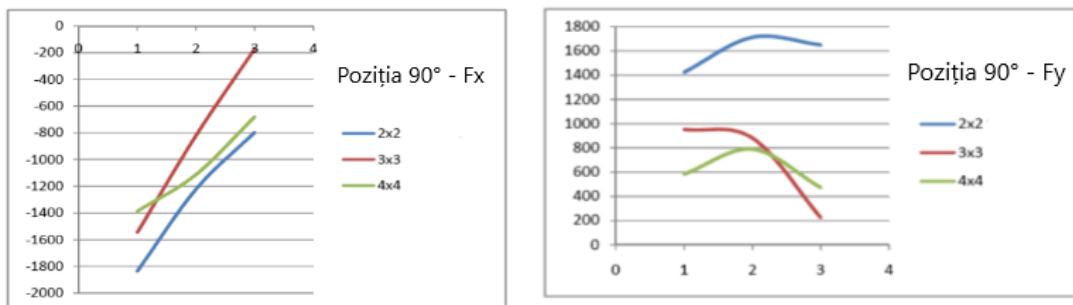


Fig. 6.22: Representation of the 3 curves given by the volumic forces: left - in the Ox direction, applied on the model of the joint positioned at an angle of 90°, which tend to attract ferrofluid to the magnets and right - in the Oy direction, which tend to resist slipping ferrofluid under the pressure forces existing in the joint

Since the dimensions of the magnets chosen after the comparative study of the volumic forces they generate are too large and wrong in terms of functionality, we tried to optimize two cases considered suitable following the second modelling study.

The two positioning variants chosen for optimization were:

- Two magnets – Case I (Figure 6.17 - a);
- Four magnets – Case I (Figure 6.17 - b).

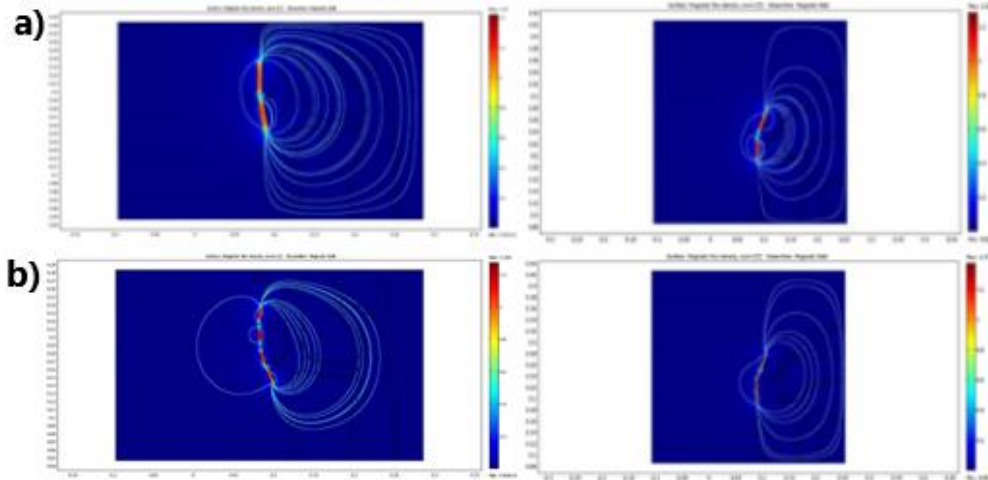


Fig. 6.23: COMSOL modeling illustrating induction and magnetic field for the two reference positions: 0° (left) and 90° (right) of the joint: a) in the case of the 2x2 matrix after the optimization process and b) in the case of the 4x4 matrix after the optimization process

Following the dimension optimization process, it can be observed that for the extreme position at 0°, the  $F_y$  volumic force for the choice of two magnets has considerably decreased its values, while the component on the  $O_x$  maintains its power at  $F_x = -473.203232$ .

Following the optimization process, in order to have the best results in the drug delivery in the patello-femoral target area, according to the results obtained after the mathematical modeling of magnets, we can conclude that we need a matrix consisting of 2 lines of 2 magnets that can be fixed near the kneecap, at distances related to the ratio:  $d1/d2 < 1$ , in order to have as much concentration of functional magnetic nanoparticles near the kneecap. To compensate for the negative values of the volumic force on the  $O_y$  axis we will choose magnets with a higher  $F_x$  component, which is achievable by increasing the remaining induction of magnet from 1.22 T to 1.42 T. The following tables show the volumic forces for each position of the knee and for each direction of action of the forces resulting from the optimization process.

Tabel 6.6: The values of the volumic forces generated following the modeling in COMSOL of the 2 cases of optimizing the configuration of the magnets for the knee joint at 0°

Conditions	Optimization for magnet 2x2	Optimization for magnet 4x4
Case I: $d1/d2 < 1$	$F_x = -473.203232$	$F_x = -19.214933$
Case II: $d1/d2 = 1$	"B = 1.42"	"B = 1.42"
Case III: $d1/d2 > 1$	$F_x = -641.068931$	$F_x = -26.031303$

<b>Case I: <math>d1/d2 &lt; 1</math></b>	$F_y = -111.376672$	$F_x = -11.09014$
<b>Case II: <math>d1/d2 = 1</math></b>	"B = 1.42" ↓	"B = 1.42" ↓
<b>Case III: <math>d1/d2 &gt; 1</math></b>	$F_y = -150.886805$	$F_y = -15.024293$

*Table 6.7: The values of the volumic forces generated following the modeling in COMSOL of the 2 cases of optimizing the configuration of the magnets for the knee joint at 90°*

<b>Conditions</b>	<b>Optimization for magnet 2x2</b>	<b>Optimization for magnet 4x4</b>
<b>Case I: <math>d1/d2 &lt; 1</math></b>	$F_x = -146.014244$	$F_x = -53.190304$
<b>Case II: <math>d1/d2 = 1</math></b>	"B = 1.42" ↓	"B = 1.42" ↓
<b>Case III: <math>d1/d2 &gt; 1</math></b>	$F_x = -197.811826$	$F_x = -72.05921$
<b>Case I: <math>d1/d2 &lt; 1</math></b>	$F_y = 145.775664$	$F_x = 39.457118$
<b>Case II: <math>d1/d2 = 1</math></b>	"B = 1.42" ↓	"B = 1.42" ↓
<b>Case III: <math>d1/d2 &gt; 1</math></b>	$F_y = 197.488611$	$F_y = 53.454269$

### 6.2.2. Testing the effect of permanent magnets on fluid with magnetic nanoparticles

With its own surface covered, magnetic nanoparticles can be dispersed into appropriate solvents to form homogeneous suspensions, so-called ferrofluids.

Magnetic nanoparticles can be coated with bioactive molecules that can interact with certain entities, monitoring their transport and release to target. They can thus be constituted in carriers of medicinal products (drugs).

Once directed and reached behind the patella, magnetic nanoparticles release the bioactive compound locally. Oral administration of proteins as such encounters a number of obstacles before being absorbed into the circulatory system. Of these can be mentioned: acid and enzyme degradation in the stomach, low permeability of the intestinal mucosa. To remove these obstacles, an attempt has been made to protect proteins (e.g. inulin) by encapsulating in hydrogels, liposomes, polymer nanoparticles.

Preliminary tests also carried out a test on an experimental model to verify whether the particles in whose matrix hyaluronic acid particles are found interact with the magnetic field source. This source is represented by the different arrangements of permanent magnets. Inulin and nanoparticles co-encapsulated in biodegradable polymer are oriented and located using a magnetic field in the knee joint area.

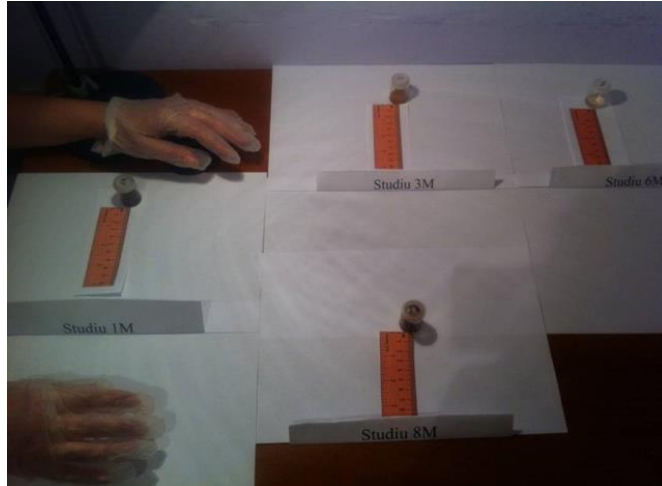


Fig. 6.24: *The location of the four solutions in order to carry out the experiment*

We've undertaken an experiment that examines whether permanent magnets can really attract magnetic particles. Thus, in Figure 6.24, the site of 4 samples with different compositions is shown.

The purpose of the application is to determine what is the retention of nanoparticles on the wall of the container near the magnets that will be placed at different sample distances.

The experiment will be based on 2 parameters:

- Time: The samples will be analyzed after 3, 10, 15 minutes after exposure to the magnetic field;
- Distance  $d$ : The magnet shall be positioned in relation to the sample at 3 mm ( $d_1$ ), 5 mm ( $d_2$ ) and 12 mm ( $d_3$ ) - Figure 6.25.

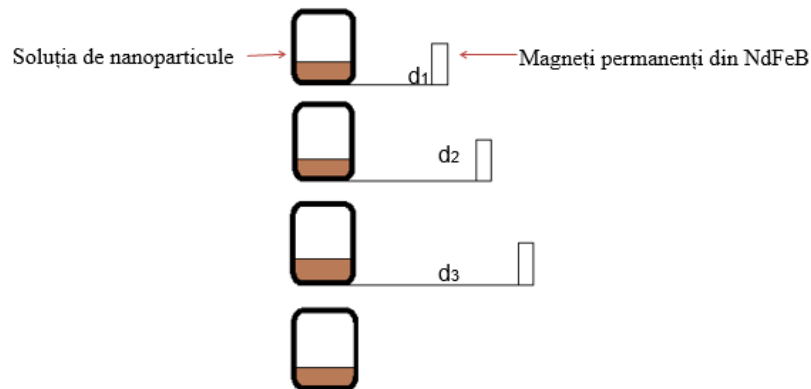
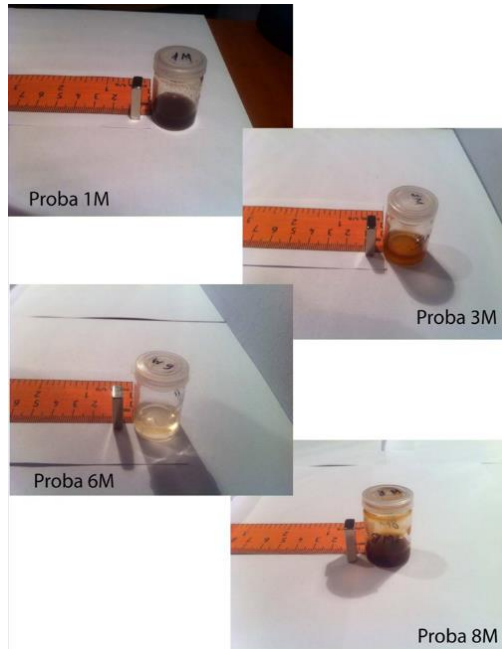


Figura 6.25: *Positioning of the samples in relation to the magnets in the case of the experimental device:  $d_1 = 3$  mm,  $d_2 = 5$  mm,  $d_3 = 12$  mm*

In order to determine the influence of the magnet on the sample, 3-time checks were carried out, following a fourth case in which the samples were left until the magnetic retention was maximum.



*Fig. 6.26: Positioning of the samples for the first stage of the experiment,  $d_2=5$  mm*

Sample 6M is the pilot sample, containing a liquid solution of sodium hyaluronate with viscoelastic properties. Magnetic nanoparticles are made up of magnetite nanoparticles, coated with inulin and then with hyaluronic acid. The last coating is biodegradable, having the property to deliver the drug. Hyaluronic acid is the medicine whose concentration should be maximum in the area behind the kneecap. Experimental solutions in number of four have a different concentration of nanoparticles (3M 1%, 1M 10% and 8M 100%). The solution contained in the 3M container is not covered consisting only of magnetic nanoparticles of magnetite and a polymer (inulin).



*Fig. 6.27: sample 1M at 15 minutes after the start of the experiment (top) and 3M sample after 35 minutes from the start of the experiment (bottom)*

All attempts were made using a permanent NdFeB magnet with dimensions of 20x10x5 mm that generates a magnetic field of 1.2 Tesla. Experimental attempts can be observed to analyse the effects of the magnetic field on the 1M sample that showed the highest magnetic retention, initially using a single magnet and then a 2x2 magnet matrix. Since the forces of attraction between magnets are very large, stabilizing them in a certain arrangement is difficult.

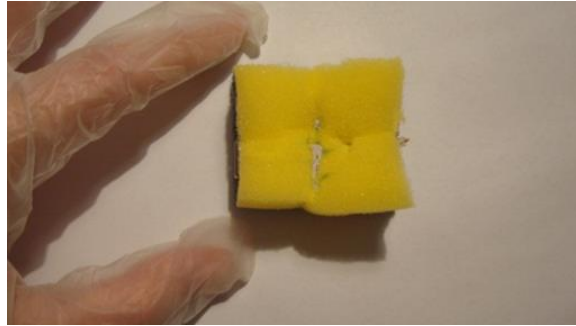


*Fig. 6.28: Configuration of two magnets per line placed in a textile support reinforced with plastic separators*

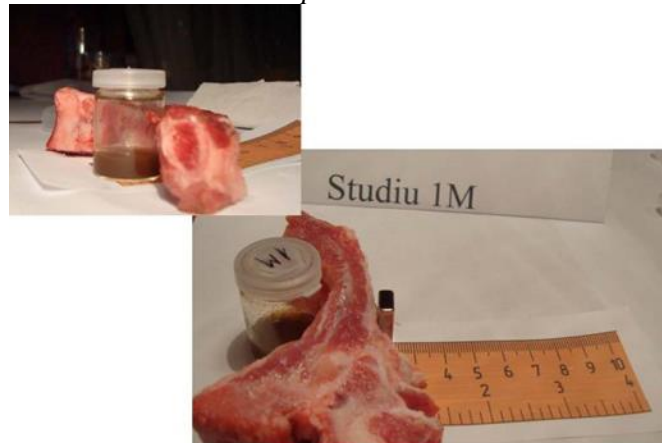


*Fig. 6.29: Simulation of the effect of a permanent magnet with dimensions of 20x10x5 mm on the ferrofluid with nanoparticles supplementing the model with a portion of tissue*

The distance between the permanent magnet and the 1M sample is corresponding to the distance  $d_3$  of the first part of the experiment in the absence of tissue material.

As the distance between the samples and the magnets increases, the number of particles decreases. After 3 minutes it can already be seen how a number of magnetic nanoparticles have accumulated on the magnet wall for 1M and 3M samples. Only a number of a few particles moved towards the walls, the movement of the others being hampered by the viscous composition of hyaluronic acid. After a 15-minute exposure, 40% was aggregated on the wall near the magnet in the 3M sample. Maintaining the two components of the device for 45 minutes will show the best magnetic retention. Sample 1M with a higher particle concentration requires a longer interaction with the magnet in order to have higher retention. The sample 8M shows no visible change, precisely because of the high concentration of nanoparticles and coatings.

Concluding, the longer the period of exposure to the magnetic field exceeds the 15-minute threshold, the more the objective of having a very good magnetic retention is met.

The introduction into the device system of a tissue with characteristics close to the application of the knee joint, will determine an obstacle that will attenuate the effect of the magnetic field and will generate the need to increase the magnet's attractiveness.

### **6.3. Testing the biocompatibility of enhanced viscoelastic solutions with drug-carrying magnetic nanoparticles**

The following experimental samples (Table 6.8) were selected for cytotoxicity tests.

Tabel 6.8: Composition of viscoelastic solutions prepared for cytotoxicity tests

Sample	Composition
Sample 1	MNP/10+HA
Sample 2	(MNP+TMOH)/10+HA
Sample 3	((MNP+TMOH)/10+inulin)+HA
Sample 4	MNP/50+HA
Sample 5	(MNP+TMOH)/50+HA
Sample 6	((MNP+TMOH)/50+inulin)+HA
Sample 7	MNP/100+HA
Sample 8	(MNP+TMOH)/100+HA
Sample 9	((MNP+TMOH)/100+inulin)+HA
Sample 10	Viscoelastic solution HA concentration 32mg/2ml

*MPN* – magnetic nanoparticles

*TMOH* – dispersing agent (tetramethylammonium hydroxide)

*INULIN* – coating agent

*HA* – hyaluronic acid

/ 10, / 50, / 100 - diluted 10, 50 or 100 times the synthetic concentration

The solutions prepared for the cytotoxicity tests were prepared and then the pH was brought to 7.4. As a reference sample (sample 10), the viscoelastic sodium hyaluronate solution with a concentration of 32 mg/2ml was used. Sterilization of experimental solutions was carried out by  $\gamma$  flash irradiation.

Biocompatibility of experimental viscoelastic solutions was evaluated using an in vitro cytotoxicity test using L929 cell culture. The test was carried out at the level of the Cantacuzino Institute. The test meets the requirements of international standards (ISO 10993-5, "Test methods for cytotoxicity - *in vitro*"). According to standard cytotoxicity testing methods, monolayers were grown at near-confluence in containers and then directly exposed to viscoelastic solutions enhanced with magnetic nanoparticles to be tested.

For this purpose, the cells were grown in modified Dulbecco Eagle (MDEM) (Sigma-Aldrich, Inc St. Louis, MO), supplemented by 10% fetal bovine serum (FBS) (BIOCHROM AG, Berlin, Germany) and 100 U/ml penicillin-streptomycin (Lonza, Verviers, Belgium) and incubated at 37°C in a humidified atmosphere of 5% CO<sub>2</sub>, in flat-down 96 plates and tissue cultures (starting concentration: 6x10<sup>5</sup> cells/ml, 100 L/well).

After incubation, the cells were exposed to dilution series of test compounds (started with 1/4) for 24 hours at 37°C in a humidified atmosphere with 5% CO<sub>2</sub>.

It should be noted from the outset that the samples diluted 10 times (sample 1, 2 and 3) were toxic to cell culture (50% cellular viability) and were removed from the study.

Samples 5, 6, 8 and 9 can be considered with a higher degree of biocompatibility because the viability of L929 cells was greater than 80%, similar to control. According to the results shown in the figure below, the samples diluted in large proportion (100) had the closest results to the reference solution (sample 10).

In terms of the type of coating used, good cellular viability results showed solutions of type (NPM + TMOH)/50 + HA and ((NPM + TMOH)/50 + Inulin) + HA. The optimal experimental sample turns out to be type ((NPM + TMOH)/50 + Inulin) + HA.

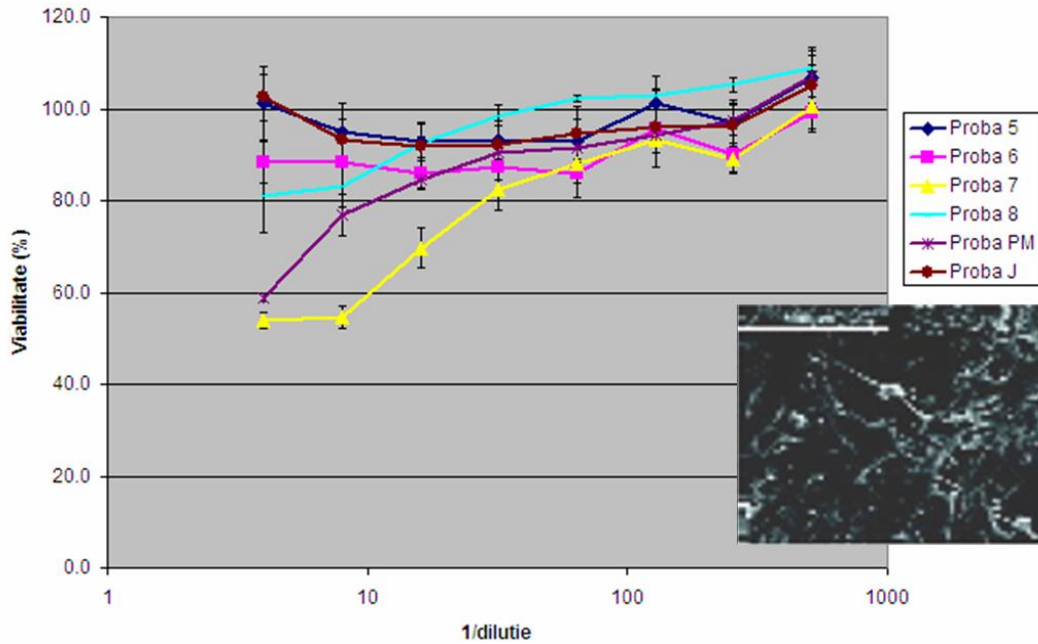


Fig. 6.30: Graphical representation of cytotoxicity test results

Thus, viscoelastic solutions with a sodium hyaluronate concentration of 32mg/2ml improved with magnetic nanoparticles of the type ((NPM + TMOH)/50 + Inulin) + HA have demonstrated the best results, both in terms of structural characteristics, rheological properties, magnetic field behaviour and biocompatibility tests, which means that all the preclinical requirements necessary in our study are met.

So, these samples can be used to make the complex kit for the treatment of joint disorders (orthosis with permanent magnets + viscoelastic solution based on sodium hyaluronate improved with magnetic nanoparticles).

## CHAPTER 7: DESIGN, EXECUTION AND PRACTICAL USE OF THE COMPLEX SYSTEM OF ORTHOSIS WITH PERMANENT MAGNETS ASSOCIATED WITH A VISCOELASTIC SOLUTION ENHANCED WITH FUNCTIONALIZED MAGNETIC NANOPARTICLES

### 7.1. Desing of orthosis with permanent magnets

The role of the orthotic device is to protect or correct the patellar position and to support and maintain the location of active permanent magnets on the femuro-patellar area. Since the device requires long periods of use, the textile pattern of the orthosis must be anatomical in order to minimally influence peripheral circulation and knee mobility. The device has been designed to allow magnets to be fixed according to the optimisation matrix. Selecting the best material is the key step in the design process.

The clinical concept from which to choose an optimal functional orthotic model is that each patient has unique needs, so that each orthosis must be customized with specifications that meet these needs. In order to achieve this, certain steps must be followed with regard to the design of an orthosis.

The first step in the selection process is to define the patient's problem in terms of instability or abnormal movement that the device needs to correct. This requires an understanding of the functional role of the knee, ligaments and capsule structures and also



This first option of designing the orthosis depends on the circumference of the knee for which it is intended, but also on the ways of fastening around the knee joint. As can be seen, the matrix of permanent magnets cannot be placed in the area of the kneecap, because of the geometry and construction of the device, since there is no supporting material in the area of the kneecap, this being discovered. These considerations lead to the conclusion that the proposed model does not meet the best functional and optimization criteria desired for the most efficient delivery of the medicines contained in the ferrite solution.

To address this design problem, a new model of femuro-patellar orthosis has been designed to encompass a larger and more localized area on the target area. Thus, the diagram in Figure 7.2. started from the same considerations as the previous orthosis to which some specific changes were added:

- The coverage as efficiently as possible of the knee joint when the mobility of the joint is maintained, and no movement constraints occur. For this purpose, an over-elastic portion was inserted behind the joint to best mimic its actual movement;
- Keeping the supporting elements positioned on either side of the knee and with a length of the segment longer than the previous model.
- The properties of the material from which the orthosis will be made will give a high degree of ease in positioning it on the knees.

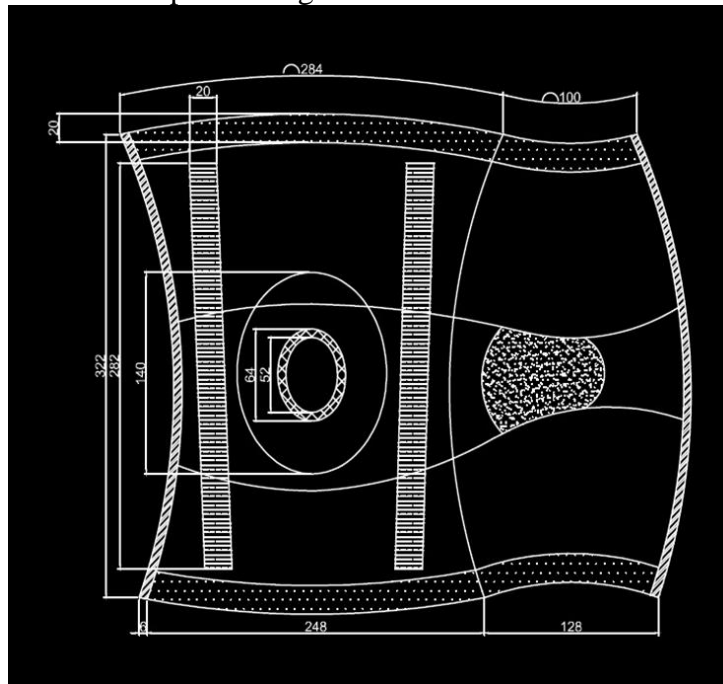


*Fig. 7.2: Scheme of designing in AutoCAD the second proposal of patelo-femoral orthosis*

The final device shall have an elastic sleeve according to the model in figures 7.3 and 7.4. It can be used in combination with a number of adjuvant devices:

- Magnets for medical use of neodymium (NdFeB – neodymium – iron – boron);
- Pressure cushions for patellar mobilization;
- Light metallic frame for biomechanical support of the pelvic limb with arthrosis damage to the knee.

The orthosis will be provided with a system of resistor structures on both compartments of the knee, through which we obtain a particularly stable orientation system - the complex of strings with integrated pressure cushions, in combination with two

corrective straps, allows stabilizing the position of the kneecap and activates the muscles, accelerating the healing process.

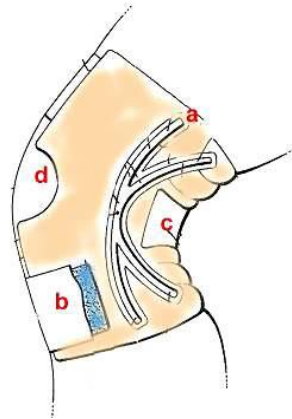


*Fig. 7.3: Profile sketch of the experimental model of femur-patellar orthosis*

The orthosis consists of the following components (Figures 7.3. and 7.4.):)

- a – the insertion area of the therapeutic magnets with a target to the internal and external femuro-patellar compartment;
- b – VELCRO elastic belt fastening system® for adjusting and pre-tensioning the orthosis;
- c – exterior cut-out to allow maximum mobility in flexion without conflict with soft tissues;
- d – adjuvant system for fixing therapeutic magnets or cushions (pad, silicone ring) for the patellar ring.



*Fig. 7.4: Images of the experimental model of the orthosis*

Summarizing the characteristics of this model, the result will be consistent with the functional requirements of the complex orthotic device with permanent magnets associated with an improved viscoelastic solution with drug-carrying magnetic nanoparticles. Due to the construction that covers the entire area of the knee joint, the magnetic component will be able to be supported in the target area, regardless of the configuration of the chosen magnets.

The knee orthosis is made of NEOPREN® on the outside and lined with hypoallergenic material on the inside, has a circular opening for centering on the kneecap and a closing system with VELCRO bands®. It is equipped with special pockets for the placement of permanent magnets of type NdFeB (code N38 and N40) in optimal positions calculated by simulating the effect of the magnetic field on magnetic nanoparticles

contained in the injected viscoelastic substance, using dedicated software packages, as previously presented.

The special design of the orthosis, the elastic material of type NEOPREN®, the way of fixing with VELCRO® bands, make it easy for the patient to tolerate and ensure the correct positioning of the magnets during treatment. The patient is instructed to wear the orthosis for as long as possible, daily, including at night, and can only remove it for activities related to personal hygiene during the 3-6 weeks of treatment.

It has previously been established that the arrangement of magnets in 4x4 matrix is the optimal position for control in the area of the femuro-patellar joint of the knee, but adaptation can be made depending on the location of the joint damage – around the kneecap for patelo-femoral damage or around each compartment (medial or lateral) in the tibio-femoral damage.

Magnetic material components, determined by experimental tests with international encodings N38, N40, have parallelepipedal shape and are adapted in a matrix of 4x4 magnets, flexible in structure according to the target area (peri-rotulian, inter-tibio-femoral, etc.). The magnetic field created concentrates (due to the properties of the biofunctional magnetic nanoparticles by coating with hyaluronate) the substance in the affected compartment where the properties of the substance are intended to be maximum and thus partially remove from the load the affected articular cartilage, giving it time for healing.

The magnets used are designed for medical use, having dimensions of the order 2-3 cm, a wide field +1000 Gauss on the surface, which allows a sufficient penetrability in human tissues (about 50 cm according to the manufacturer's specifications). The number, dimensions and location of the magnets, as well as the resonant induction of the magnetic field created by them, were determined by analyses carried out with software programs dedicated to the modeling and analysis of the magnetic field in the earlier stages of this work.

## 7.2. How to clinically use the complex system

With regard to the practical use of the complex system of orthosis with permanent magnets associated with an improved viscoelastic solution with magnetic nanoparticles bearing the drug, this subchapter presents the clinical method of therapy of joint disorders based on the effect of the magnetic field and controlled viscosupplementation.

Thus, the therapeutic kit contains the following components (Figure 7.5):

- Fiola with sterile viscoelastic substance with magnetic nanoparticles coated with hyaluronic acid;
- Mobile knee orthosis with magnets for therapeutic use NdFeB.

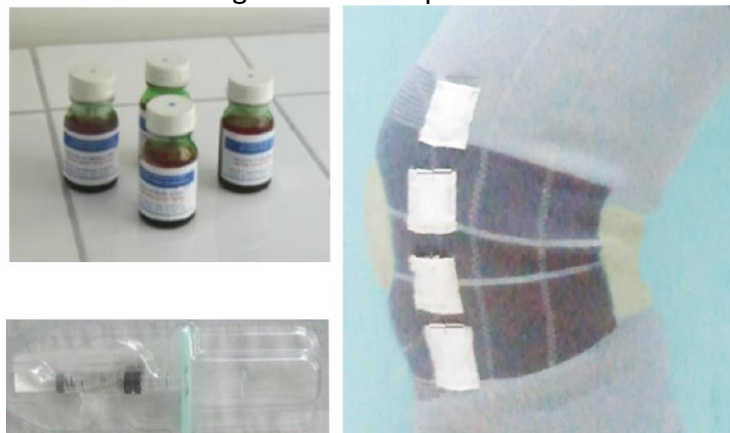


*Fig. 7.5: Components of the therapeutic kit of the complex system of orthosis with permanent magnets associated with improved viscoelastic solution with magnetic nanoparticles carrying the drug*

The following will detail the working protocol for the use, in medical practice, of magnetically controlled viscosupplementation. The following clinical method shall be developed, including the following stages:

### **1. Specifying the topography and depth of the cartilaginous lesion**

It is made using the following methods:

- Clinical methods (precise anamnesis, which specifies the location of pain, circumstances of triggering and worsening of pain, evolution over time);
- Radiological methods: bilateral knee x-ray anteroposterior incidence, in load and flexion of 30 degrees, bilateral profile X-ray;
- Imaging methods: MRI examination of the knee, arthroscopic methods: arthroscopic examination of the knee with indication of topography and depth of the lesion, in accordance with internationally accepted classifications (Outerbridge, ICRS). Arthroscopic images will be stored and compared to the results of minimally invasive arthroscopic examination (optical minimum 1,6 mm) post-therapy.

At the end of stage 1 the affected area with dimensions and degrees of depth is explicitly known and a data sheet can be drawn up with these data representing the control with which, at the end of treatment, the results of the use of magnetically controlled viscosupplementation are evaluated and at the same time the area in which magnets are fixed during treatment, is established in order to achieve optimal clinical results.

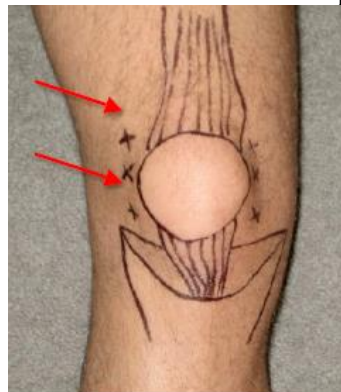


*Fig. 7.6: Clinical image showing the area of interest for the application of the orthosis therapeutic kit with permanent magnets*

### **2. Injection of the viscoelastic substance containing nanoparticles**

Depending on the result of the previous stage, choose the compartment in which the intra-articular injection is made internal, external or femuro-patellar.

The patient's position is in the dorsal decubit, with the knee in flexion of 70°-90° for the internal or external compartment and in the dorsal decubit with the knee in flexion of about 30° in the case of the femuro-patellar compartment. The knee is prepared by brushing with an antiseptic substance (betadine solution 10%). The doctor injecting the substance should be familiar with the anatomy of the region, in order to avoid puncture of vessels, nerves or tendon structures in the respective area.

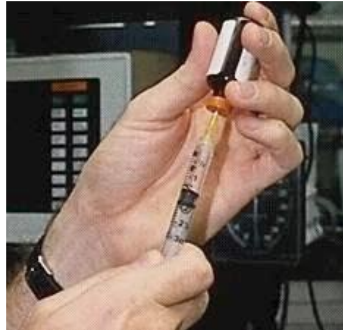


*Fig. 7.7: Injectable viscoelastic solution used*

Prior to injection, general contraindications of the administration of viscoelastic substances should be excluded, namely: active skin lesions, dermatitis, known bacteremia, diagnosed periarticular osteomyelitis, uncontrolled coagulopathy, the presence of a permanent implant - arthroplasty with total knee prosthesis.

The anatomical markers shall be established in relation to which the injection of the substance will be carried out. These are:

- Lateral edge of the kneecap,
- Lower edge of the kneecap,
- Medial and lateral edges of the patellar tendon,
- The level of the articular interline (Fig. 7.8).



*Fig. 7.8: Injection of the viscoelastic solution at the level of the articular interline (schematic representation)*

Landmarks can be drawn prior to the procedure with a marker (Fig. 7.6).

For injection into the femuro-patellar compartment, use the para-patellar approach, with the knee in flexion of 10°. The entry point is located 3 mm below the half of the lateral face of the kneecap and the needle is positioned perpendicular to the femur and in the direction of the intercondilian space.

An infra-patellar approach with the knee in 90° flexion is used for injection into the internal or external compartment.

The entry point of the needle is in the triangle bounded by the limit of 5 mm lower than the lower edge of the kneecap and the lateral/medial edges of the patellar tendon (Figure 7.9); hence the needle is directed towards the intercondilian space. It is covered the knee with antiseptic solution and wait 30 seconds for drying the solution. Local anesthesia is optional but should be considered for patient comfort. It is carried out by injecting an anesthetic substance of type xiline 0,5%, 1,5-3 ml, strictly into the subcutaneous tissue. Any deep injection will be avoided as it may alter the qualities of the joint fluid. After injection of the anesthetic substance, an interval of 1-2 minutes will be expected to be installed. Throughout the procedure, the medical is equipped with sterile gloves.

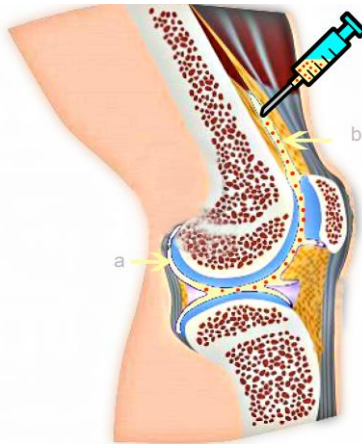


*Fig. 7.9: Scheme of technical principle - stage I in which, at the time of injection, the viscoelastic fluid functionalized with nanoparticles (b) is diluted in the synovial fluid*

The substance is conditioned in sterile vial and sterile packed. The assistant unpacks the package and presents the doctor's vial. It takes it over and examines it - the solution must be clear, have no deposits, sediments or colour changes and be within the shelf life of sterilization. If these conditions are met, then a sterile needle (no.25-27 with a length of 5-6 cm) is then adapted to the syringe of 2ml capacity. Guided by the points specified above, insert the needle and vacuum; the presence of a minimum amount of intra-articular fluid (clear yellow citron) in the syringe, confirms the intra-articular positioning of the needle. From this point on, the viscoelastic substance with nanoparticles is introduced slowly, progressively (rapid introduction of the substance may cause a sudden increase in intra-articular pressure and may trigger intense pain to the patient). When all viscoelastic substance with nanoparticles has been inserted, the needle is removed, the site of the joint puncture is covered with disinfectant and a sterile dressing is applied for 24 hours. The patient is instructed not to maintain a position in prolonged orthostatism or clinostatism on the day of injection in order not to cause inflammation of the synovial and determination of a reaction that reduces the effect of the viscoelastic substance. Return to the usual activities is progressively allowed from the day after injection.

### **3. Aplicarea ortezei prevazută cu magneți**

Depending on the outcome of the full examination in point 1, the orthosis is provided with permanent magnets for medical use NdFeB, the purpose of which is to concentrate, due to the magnetic properties of the nanoparticles, the substance in the affected compartment, the one in which the properties of the viscoelastic substance are intended to be maximum and thus to remove, in part, from the loading of the affected articular cartilage and give it time to repair. NdFeB magnets are arranged in line, in specially created pockets in the orthosis, so as to ensure the concentration of the substance in the affected compartment. The patient is instructed to wear orthotics for as long as possible daily, including at night.



*Fig. 7.10: Stage II, in which, by applying the permanent magnet orthosis, a concentration effect of the magnetic nanoparticles coated with sodium hyaluronate on the femoral-patellar target area is obtained*

Orthosis can only be removed for activities related to personal hygiene during the 3 to 6 weeks of treatment. The special design of the orthosis makes it easy for the patient to tolerate and ensures the correct positioning of the magnets during treatment. Positioning is easily done when the defining anatomical elements are respected:

- anterior - patellar relief,
- posterior - flexion fold of the knee joint.

No restrictions are required on physical activity other than those related to possible surgery performed prior to the start of treatment.



*Fig. 7.11: Design of the final complex system of orthosis with permanent magnets*

#### **4. Patient supervision during treatment**

The patient is required to report for check-up at 24 hours and 72 hours; during these examinations we ensure that the patient tolerates well the injected substance and the orthosis is in the correct position. Subsequently the patient is reviewed - as far as possible - weekly. During these checks the patient will be questioned on his perception of therapy: if it is considered that there is a degree of pain relief, if his physical activity has improved.

#### **5. Appreciation of the final result of the treatment**

The final result will be assessed on the basis of objective criteria, as follows:

a) Arthroscopic criteria: refer to the minimally invasive Inerview examination, which allows with the help of a probe of 1.6 to 1.8 mm size to explore the interior of the knee joint, in a procedure which does not involve a type of anesthesia other than local and which can be performed in a specialized ambulatory regime. All video images obtained will be stored and compared with those obtained in point 1. From their comparison, the

effectiveness of the procedure can be deduced (according to ICRS – International Cartilage Research Society Score).

b) Anatomic-pathological criteria: whenever the patient agrees, a minimum amount of articular cartilage will be harvested (during the same In vivo examinations), with the help of a trephine with a diameter of 2 mm. Its histological examination will allow the quantitative assessment of the repaired hyaline cartilage or the obtained fibrocartilage.

c) Imaging criteria: whenever possible (preferably in all cases) an MRI image of the knee will be obtained 6 to 12 months after initiation of treatment and will be compared with the MRI image prior to treatment.

d) Clinical criteria: involve objective evaluation of the patient's symptomatology compared to that prior to treatment. Consideration will be given to: cracks, spontaneous and stress-induced pain, the degree of exertion at which pain occurs, improvement of post-treatment physical performance, stability of these improvements over time; so the patient will be examined at 6 weeks, 3 months, 6 months, 1 year and then annually.

In order to ensure the patient's compliance, he will be informed at the time of joining the lot that it is a new procedure, the viability of which is in the documentation and for this reason it will need to be examined repeatedly.

## **C1. GENERAL CONCLUSIONS**

---

From the analysis of the present doctoral thesis, the following general conclusions and assessments can be deduced:

Functionalized magnetic nanoparticles possess several special advantages that make them tempting for use in medical field by their ability to direct drugs in the human body with the help of the magnetic field, both in the area of medical imaging, due to the ability to incorporate fluorescent substances and medical treatments and in the field of medical treatments, due to the ability to incorporate and transport drugs.

However, it is not easy to develop medical applications of functionalized magnetic nanoparticles due to potential toxicity issues as well as knowledge of the mechanisms of interaction and functionality in the human body.

Most of the functionalized magnetic nanoparticles with applicability in medicine that have been investigated so far have been those used in the field of medical imaging. Relatively recently, attempts have been made to develop functionalized magnetic nanoparticles carrying drugs for the treatment of various diseases. The main impediment in the development of these applications is that after fulfilling their functional role they are difficult to eliminate and the mechanism by which they subsequently move in the human body or how it influences human metabolism is not elucidated.

Iron oxide particles are the preferred magnetic nanoparticles due to their superparamagnetism and anisotropy; they also have a hydrophobic surface, a high saturation field, high field irreversibility and, more importantly, a high load that allows them to remain stable in the body under physiological conditions. The size of the nanoparticles is decisive in terms of their magnetic properties and the encapsulation of the cells.

At this time, there is a high incidence of osteo-articular diseases among the population. Current treatment solutions involve, depending on the type of disease and the degree joint degradation, the use of different orthoses models to stabilize the joints, the use of viscoelastic solutions to ensure joint lubrication, associated or not with drug treatment.

The viscosupplementary treatment, basically, it consists of repeated intra-articular injections with hyaluronic acid, which is used to obtain beneficial hydrogels for tissue regeneration, due to the high biocompatibility.

The use of functionalized magnetic nanoparticles is necessarily associated with an external magnetic field, generated by permanent magnets. For the treatment of osteo-articular diseases, it is very effective to use an orthosis with permanent magnets to ensure the movement and stabilization of the magnetic nanoparticles carrying the drug in the area of affected tissues.

The design of a complex system of functionalized magnetic nanoparticles used in a viscoelastic solution associated with an orthosis with permanent magnets, for the treatment of osteo-articular diseases requires interdisciplinary knowledge of materials, magnetic field, biomechanics, biochemistry, modeling and simulation, medicine.

The synthesis of magnetic nanoparticles is easily accomplished by chemical methods, such as the co-precipitation of ferric chloride and ferrous chloride. This method provides satisfactory results.

The functionalization of nanoparticles is usually done with polymeric materials, because they improve their biocompatibility and operating properties. These functionalizing materials can have a therapeutic role, as in the case of hyaluronic acid, providing special biological and chemical properties to magnetic nanoparticles.

To test and evaluate such a complex system, the use of magnetic nanoparticle analysis techniques is required methods for testing viscoelastic solutions, programs for simulating magnetic properties to determine the optimal position of magnets and last but not least testing the biocompatibility by cytotoxicity tests of these materials.

---

## **C2. ORIGINAL CONTRIBUTIONS**

---

The research carried out brought a series of contributions as a novelty through the original results obtained and through their theoretical interpretation.

The original contributions will be presented below along with the most important results obtained.

A complex synthesis of the scientific documentation was performed, which led to the obtaining of many new results and interpretations, some of them being novel and original.

As a result of the complex literature study performed, criteria have been established for the selection of materials usable for the execution of the complex system of orthosis with permanent magnets associated with an improved viscoelastic solution with functionalized magnetic nanoparticles.

An application of drug-carrying functionalized magnetic nanoparticles with applicability in the treatment of osteo-articular diseases has been identified and developed. The major advantage of this application is that the nanoparticles can be removed by a simple aspiration after fulfilling their role of controlled delivery of the drug in the affected osteo-articular area.

New functionalized MNPs with tetramethylammonium hydroxide (TMOH), inulin and hyaluronic acid have been successfully obtained, which have the role of providing uniformity, homogeneous distribution, optimal nanoparticle size and outstanding biocompatibility. Moreover, hyaluronic acid has a therapeutic role in osteo-articular diseases, which means that these nanoparticles are recommended for medical use.

The functionalization of MNPs was performed by the layer-by-layer method, initially with a TMOH layer, which provides homogeneous distribution to the nanoparticles, then with an inulin layer and a hyaluronic acid layer, which helps to fulfill the therapeutic role of these nanoparticles.

Scanning electron microscopy (SEM), transmission electron microscopy (TEM), Fourier transform infrared spectroscopy (FT-IR), dynamic light scattering (DLS) studies have allowed a detailed characterization of MNPs.

Simulation and modeling research on the magnetic properties of MNPs when interacting with an external magnetic field using the COMSOL program was performed.

The design of the optimal orthosis model with permanent magnets was successfully performed in the AutoCAD program.

Cytotoxicity tests were performed, which demonstrated that the experimental materials are biocompatible and usable in the treatment of osteo-articular diseases. Obviously, it is necessary to perform complete in vitro and in vivo biocompatibility tests in the future.

The set of studies allows us to conclude that the main objective of the doctoral thesis was met, respectively a complex system of permanent magnet orthosis was obtained associated with an improved viscoelastic solution with functionalized MNPs to meet the functional requirements of their use in osteo-articular diseases treatment.

Based on the experimental results obtained, it can be said that MNPs functionalization has much better results when using the coating with three different layers, namely with TMOH, inulin and HA.

It is mentioned that the experimental part was performed mainly in the laboratories of the Department of Metallic Materials Science and Physical Metallurgy, Faculty of Materials Science and Engineering, Polytechnic University of Bucharest, but experimental determinations were performed in other laboratories.

The synthesis of MNPs and their functionalization was carried out in collaboration with the ICECHIM Institute, Bucharest under the coordination of Mr. Cristian Petcu.

Also, a series of experimental determinations were performed at the Polytechnic University of Bucharest in collaboration with: Mr. Alexandru Morega from the Faculty of Electrical Engineering, Polytechnic University of Bucharest for simulation in the COMSOL program, with Mr. Balan Corneliu for rheology tests and with Ms. Diana Popescu from the Faculty of Industrial and Robotic Engineering, for the design of the device.

Far from claiming to exhaust the theoretical and experimental research in the field of functionalized MNPS for medical applications, the paper makes a theoretical and practical contribution, while opening new horizons for future research in this field.

---

### **C3. PERSPECTIVES FOR FURTHER DEVELOPMENT**

---

This doctoral thesis has prospects for further development in several directions.

Thus, it is possible to extend the studies on the role played by the magnetic field on the efficiency of the magnet orthosis and to follow the evolution of MNP at the joints depending on the use of the magnet orthosis.

Further research on the improvement of MNP functionalization methods can be developed by adding other coatings (specific proteins or growth factors).

Obviously, it is possible to expand research on in vitro and in vivo biocompatibility testing in specific animal models.

## SELECTIVE BIBLIOGRAPHY

---

- [1] *Osama A., Humza O., Joel M.*, Biomechanics of the knee, *Orthopaedics and Trauma*, vol. 33, 2019, p. 224-230.
- [2] *Alice J. S. Fox, Asheesh B., Scott A. R.*, The Basic Science of Human Knee Menisci Structure, Composition, and Function, *Sports Health*, vol. 4, 2012, p. 340–351.
- [3] *Hunziker E.B.*, Articular cartilage repair: basic science and clinical progress. A review of the current status and prospects, *Osteoarthritis and Cartilage*, vol. 10, 2002, p. 432-463.
- [4] *Tan K., Hammond E.R., Kerr D., Nath A.*, Fibrocartilaginous Embolism: A Cause of Acute Ischemic Myelopathy, *Spinal Cord*, vol. 47, 2009, p. 643-5.
- [5] *McCarty W. J., Masuda K., Sah R. L.*, Fluid movement and joint capsule strains due to flexion in rabbit knees, *Journal of Biomechanics*, vol. 44, 2011, p. 2761-2767.
- [6] *Wyatt L. A., Nwosu L. N., Wilson D., Spendlove I., Bennett A. J., Scammell B. E., Walsh D. A.*, Molecular expression patterns in the synovium and their association with advanced symptomatic knee osteoarthritis, *Osteoarthritis and Cartilage*, vol 27, 2019, p. 667-675.
- [7] *Carlson A. K., Rawle R. A., Wallace C.W., Brooks E.G., Greenwood M.C., Olmer M., Lotz M. K., Bothner B., June R. K.*, Characterization of synovial fluid metabolomic phenotypes of cartilage morphological changes associated with osteoarthritis, *Osteoarthritis and Cartilage*, Vol. 27, 2019, p. 1174-1184.
- [15] *Gold P. A., Jones M. R., Kaye A. D.*, Chapter: Knee Joint Pain., Springer Nature Switzerland AG, 2019, p. 761–765.
- [16] *Qassim I., Muaidi L., Nicholson L., Kathryn M.*, Proprioceptive Acuity in Active Rotation Movements in Healthy Knees, *Archives of Physical Medicine and Rehabilitation*, vol. 89, 2008, p. 371-376.
- [17] *Charles A., Baumann B. S., Betina B. H., Miho J. T.*, Update on Patellofemoral Anatomy and Biomechanics, *Operative Techniques in Sports Medicine*, vol. 27, 2019, p. 150683.
- [26] *Patrick K. S., Wendy M. N., DStephen J. N., James A. B.*, Increasing Public Interest in Stem Cell Injections for Osteoarthritis of the Hip and Knee: A Google Trends Analysis, *The Journal of Arthroplasty*, vol. 34, 2019, p. 1053-1057.
- [27] *Tuuli S., Lars C., Jón K., Johan K.*, Knee kinematics in medial arthrosis. Dynamic radiostereometry during active extension and weight-bearing, *Journal of Biomechanics*, vol. 38, 2005, p. 285-292.
- [28] *Dejour H. G., Walch G. Deschamps P. C.*, Arthrosis of the knee in chronic anterior laxity, *Orthopaedics & Traumatology: Surgery & Research*, vol. 100, 2014, p. 49-58.
- [29] *Brian R. H.*, Treatment of Knee Arthrosis in the Morbidly Obese Patient, *Orthopedic Clinics of North America*, vol. 42, 2011, p. 107-113.
- [30] *Hideki S., Yasuyuki I., Eiichi T., Kazuhiro S., Satoshi T.*, Total knee arthroplasty for gonarthrosis with patellar dislocation, *Journal of Orthopaedic Science*, vol. 10, 2005, p. 656-660.
- [33] *Chamarda H. A., Carriera N., Duforta P., Duranda M., Brum-Fernandes A.J., Boirea G., Komarovab S.V., Dixonc S. J., Harrisond R. E., Manolsone M.F., Rouxa S.*, Osteoclasts and their circulating precursors in rheumatoid arthritis: Relationships with disease activity and bone erosions, *Bone Reports*, vol. 12, 2020, 100282.
- [35] *Shing T. L., Peter C. T.*, Role of biological agents in treatment of rheumatoid arthritis, *Pharmacological Research*, vol. 150, 2019, 104497.
- [40] *Hunt M. A., Charlton M., Esculier F.*, Osteoarthritis year in review 2019: mechanics, *Osteoarthritis and Cartilage*, vol. 28, 2020, p. 267-274.

- [49] *Yong W. L., Mark D. T., Matthew R. S., Dakshesh B. P., Eric A. W., Anderanik T., Jordan S. G., Thomas V., George R. M.*, MR imaging of cartilage repair surgery of the knee, *Clinical Imaging*, vol.58, 2019, p. 129-139.
- [50] *Dae-Hee L., Darry D., D’Lima S., Hak L.*, Clinical and radiographic results of partial versus total meniscectomy in patients with symptomatic discoid lateral meniscus: A systematic review and meta-analysis, *Orthopaedics & Traumatology: Surgery & Research*, vol. 105, 2019, p. 669-675.
- [51] *Petersen W., Zantop T.*, Partial rupture of the anterior cruciate ligament, *Arthroscopy*, vol. 22, 2006, p. 1143-1145.
- [52] *Guenoun D., Le Corroller T., Amous Z., Pauly V., Sbihi A., Champ-saur P.*, The contribution of MRI to the diagnosis of traumatic tears of the anterior cruciate ligament, *Diagnostic and Interventional Imaging*, vol. 93, 2012, p. 331-341.
- [53] *O’Keeffe A. S., Brian A. H., Stephen J. E., Eoin C .K.*, Overuse Injuries of the Knee, *Magnetic Resonance Imaging Clinics of North America*, vol. 17, 2009, p. 725-739.
- [67] *Allan R., Woodburn J., Telfer S., Abbott M., Steultjens M. P.*, Knee joint kinetics in response to multiple three-dimensional printed, customised foot orthoses for the treatment of medial compartment knee osteoarthritis, *Proceedings of the Institution of Mechanical Engineers-Part H*, vol. 231, 2017, p. 487–498.
- [72] *Florina D.C., Vera B., Marcel I.P., Andrei L., Aurora A., Iulian V.A., Liliana V.*, Biopolymers – Calcium Phosphates Composites with Inclusions of Magnetic Nanoparticles for Bone Tissue Engineering, *International Journal of Biological Macromolecules*, vol. 125, 2019, p. 612-620.
- [76] *Vasvani S., Kulkarni P., Rawtani D.*, Hyaluronic acid: A review on its biology, aspects of drug delivery, route of administrations and a special emphasis on its approved marketed products and recent clinical studies, *International Journal of Biological Macromolecules*, vol. 151, 2020, p. 1012-1029.
- [78] *Rau J. V., Antoniac, I., Cama, G., Komlev, V. S., Ravaglioli, A.*, Bioactive Materials for Bone Tissue Engineering, *BioMed Research International*, 2016, p. 1–3.
- [79] *Iulian A., Dan L., Camelia T., Claudia M., Sebastian G.*, Osteochondral Tissue Engineering, Chapter 12, *Synthetic Materials for Osteochondral Tissue Engineering*, Springer International Publishing AG, 2018, p. 31-52.
- [86] *Conroy S., Jerry S.H. L., Miqin Z.*, Magnetic nanoparticles in MR imaging and drug delivery, *Advanced Drug Delivery Reviews*, vol. 60, 2008, p. 1252-1265.
- [92] *Sasso C. P., Basso V., LoBue M., Bertotti G.*, Carnot cycle for magnetic materials: The role of hysteresis, *Physica B: Condensed Matter*, vol. 372, 2006, p. 9–12.
- [93] *Allia P., Barrera G., Tiberto P.*, Hysteresis effects in magnetic nanoparticles: A simplified rate-equation approach, *Journal of Magnetism and Magnetic Materials*, vol. 496, 2020, 165927.
- [94] *Shokrollahi H., Janghorban K.*, Soft magnetic composite materials (SMCs), *Journal of Materials Processing Technology*, vol. 189, 2007, p. 1–12.
- [95] *Ucar H., Choudhary R., Paudyal D.*, An Overview of the First Principles Studies of Doped RE-TM5 Systems for the Development of Hard Magnetic Properties, *Journal of Magnetism and Magnetic Materials*, vol. 496, 2020, 165902.
- [96] *Ríos Á., Zougagh M.*, Recent advances in magnetic nanomaterials for improving analytical processes, *TrAC Trends in Analytical Chemistry*, vol. 84, 2016, p. 72–83.
- [100] *Coey J. M. D.*, Perspective and Prospects for Rare Earth Permanent Magnets, *Engineering*, vol. 6, 2020, p. 119-131
- [101] *Croat J. J., Herbst J. F., Lee, R. W., Pinkerton F. E.*, Pr-Fe and Nd-Fe-based materials: A new class of high-performance permanent magnets, *Journal of Applied Physics*, vol. 55, 1984, p. 2078–2082.

- [108] *Choi B., Park W., Park S. B., Rhim W. K., Keun H. D.*, Recent trends in cell membrane-cloaked nanoparticles for therapeutic applications, *Methods*, vol. 117, 2020, p. 2-14.
- [109] *Wang B., Sandre O., Wang K., Shi H., Xiong K., Huang Y., Courtois, J.*, Auto-degradable and biocompatible superparamagnetic iron oxide nanoparticles/polypeptides colloidal polyion complexes with high density of magnetic material, *Materials Science and Engineering: C*, vol. 104, 2019, 109920.
- [111] *Sudarsana Reddy P., Chamkha A. J.*, Influence of size, shape, type of nanoparticles, type and temperature of the base fluid on natural convection MHD of nanofluids, *Alexandria Engineering Journal*, vol. 55, 2016, p. 331–341.
- [112] *Khan A. I., Arasu A. V.*, A review of influence of nanoparticle synthesis and geometrical parameters on thermophysical properties and stability of nanofluids, *Thermal Science and Engineering Progress*, vol. 11, 2019, p. 334-364.
- [115] *Hojin K., Eric M. F.*, Magnetic properties, responsiveness, and stability of paramagnetic dumbbell and ellipsoid colloids, *Journal of Colloid and Interface Science*, vol. 566, 2020, p. 419-426.
- [116] *Mottaghitlab F., Farokhi M., Fatahi Y., Atyabi F., Dinarvand R.*, New insights into designing hybrid nanoparticles for lung cancer: Diagnosis and treatment, *Journal of Controlled Release*, vol. 295, 2019, p. 250-267.
- [119] *Kudr J., Haddad Y., Richtera L., Heger Z., Cernak M., Adam V., Zitka O.*, Magnetic Nanoparticles: From Design and Synthesis to Real World Applications. *Nanomaterials*, vol. 7, 2017, p. 243.
- [120] *Čubová K., Čuba V.*, Synthesis of inorganic nanoparticles by ionizing radiation – a review. *Radiation Physics and Chemistry*, vol. 164, 2020, 108774.
- [122] *Israel L. L., Galstyan A., Holler E., Ljubimova J. Y.*, Magnetic iron oxide nanoparticles for imaging, targeting and treatment of primary and metastatic tumors of the brain, *Journal of Controlled Release*, vol. 320, 2020, p. 45-62.
- [123] *Aisida S. O., Akpa P. A., Ahmad I., Zhao T., Maaza M., Ezema F. I.*, Bio-inspired encapsulation and functionalization of iron oxide nanoparticles for biomedical applications, *European Polymer Journal*, vol. 122, 2019, 109371.
- [125] *Elrahman A. A., Mansour F. R.*, Targeted magnetic iron oxide nanoparticles: Preparation, functionalization and biomedical application, *Journal of Drug Delivery Science and Technology*, vol. 52, 2019, p.702-712.
- [126] *Regina R. G., López A. C., Serna Gómez I., Campos D. S., Otero-González A. J., Luiz Franco O.*, Antimicrobial magnetic nanoparticles based-therapies for controlling infectious diseases, *International Journal of Pharmaceutics*, vol. 555, 2019, p. 356-367.
- [127] *Maudens P., Jordan O., Allémann E.*, Recent advances in intra-articular drug delivery systems for osteoarthritis therapy, *Drug Discovery Today*, vol. 23, 2018, p. 1761-1775.
- [135] *Xue Z.W., Lande L., Rui F. L., Richard J. T., Ken P., Jason C., Fraser K. McNeil-Watson*, Online characterisation of nanoparticle suspensions using dynamic light scattering, ultrasound spectroscopy and process tomography, *chemical engineering research and design*, vol. 87, 2009, p. 874–884.
- [141] *Vandna P., Prajakta D., Ratnesh J.*, Nanoparticulate drug delivery, Chapter 4: Nanotoxicology: evaluating toxicity potential of drug-nanoparticles, Woodhead Publishing Limited, 2012, p. 123-155.
- [142] *Iulian A., Alexandru C., Cristian P., Dan L., Diana T., Camelia T., Aurora A., Sebastian G.*, Synthesis and Characterization of Coated Iron Oxide Nanoparticles Produced for Drug Delivery in Viscoelastic Solution, *Revista de Chimie*, vol. 71, 2020, p. 145-154. *Revista de Chimie*, vol. 71, 2020, p. 145-154.